1404 *Inorg. Chem.* **2010**, *49*, 1404–1419
DOI: 10.1021/ic901431r

Inorganic Chemistry
Article

Reductive Coupling of Nitrogen Monoxide (•NO) Facilitated by Heme/Copper Complexes

Jun Wang,[†] Mark P. Schopfer,[†] Simona C. Puiu,[†] Amy A. N. Sarjeant,[†] and Kenneth D. Karlin*[,†,‡]

[†]*Department of Chemistry, The Johns Hopkins University, Baltimore, Maryland 21218 and* [‡]*Department of Bioinspired Science, Ewha Womans University, Seoul 120-750, Korea*

Received July 21, 2009

The interactions of nitrogen monoxide (•NO; nitric oxide) with transition metal centers continue to be of great interest, in part due to their importance in biochemical processes. Here, we describe $\bullet NO_{(g)}$ reductive coupling chemistry of possible relevance to that process (i.e., nitric oxide reductase (NOR) biochemistry), which occurs at the heme/Cu active site of cytochrome *c* oxidases (C*c*Os). In this report, heme/Cu/$\bullet NO_{(g)}$ activity is studied using 1:1 ratios of heme and copper complex components, $(F_8)Fe$ (F_8 = tetrakis(2,6-difluorophenyl)porphyrinate(2-)) and $[(tmpa)Cu^{I}(MeCN)]^{+}$ (TMPA = tris(2-pyridylmethyl)amine). The starting point for heme chemistry is the mononitrosyl complex $(F_8)Fe(NO)$ (λ_{max} = 399 (Soret), 541 nm in acetone). Variable-temperature ^1H and ^2H NMR spectra reveal a broad peak at δ = 6.05 ppm (pyrrole) at room temperature (RT), which gives rise to asymmetrically split pyrrole peaks at 9.12 and 8.54 ppm at −80 °C. A new heme dinitrosyl species, $(F_8)Fe(NO)_2$, obtained by bubbling $(F_8)Fe(NO)$ with $\bullet NO_{(g)}$ at −80 °C, could be reversibly formed, as monitored by UV−vis (λ_{max} = 426 (Soret), 538 nm in acetone), EPR (silent), and NMR spectroscopies; that is, the mono-NO complex was regenerated upon warming to RT. $(F_8)Fe(NO)_2$ reacts with $[(tmpa)Cu^{I}(MeCN)]^{+}$ and 2 equiv of acid to give $[(F_8)Fe^{III}]^{+}$, $[(tmpa)Cu^{II}(solvent)]^{2+}$, and $N_2O_{(g)}$, fitting the stoichiometric $\bullet NO_{(g)}$ reductive coupling reaction: $2\bullet NO_{(g)} + Fe^{II} + Cu^{I} + 2H^{+} \rightarrow N_2O_{(g)} + Fe^{III} + Cu^{II} + H_2O$, equivalent to one enzyme turnover. Control reaction chemistry shows that both iron and copper centers are required for the NOR-type chemistry observed and that, if acid is not present, half the •NO is trapped as a $(F_8)Fe(NO)$ complex, while the remaining nitrogen monoxide undergoes copper complex promoted disproportionation chemistry. As part of this study, $[(F_8)Fe^{III}]SbF_6$ was synthesized and characterized by X-ray crystallography, along with EPR (77 K: g = 5.84 and 6.12 in CH_2Cl_2 and THF, respectively) and variable-temperature NMR spectroscopies. These structural and physical properties suggest that at RT this complex consists of an admixture of high and intermediate spin states.

Introduction

In this report, we describe the reductive coupling of 2 mol equiv of nitrogen monoxide ($\bullet NO_{(g)}$; nitric oxide) to nitrous oxide ($N_2O_{(g)}$), $2\bullet NO_{(g)} + 2\ H^{+} + 2\ e^{-} \rightarrow N_2O_{(g)} + H_2O$, mediated by a heme plus copper complex in the presence of acid. The particular compounds employed and the overall reaction discussed are shown in Scheme 1. This follows our previous paper[1] on similar chemistry carried out by a binuclear heme/Cu assembly possessing a binucleating ligand. That was the first example of such chemistry with heme/Cu, modeling the heterobinuclear center present at the active site of cytochrome *c* oxidase (C*c*O).

In fact, bacterial •NO reductases (NORs) effect this reductive coupling of •NO, and these have a related active site, a heme with a proximate nonheme iron metal center.[2−4] Actually, these two enzyme classes are evolutionarily related.[5,6] The heme/M (M = Fe or Cu) centers both possess a number of conserved histidines: one is a proximal ligand for the heme of the binuclear heme/M center (as in hemoglobin/myoglobin), and three other histidine imidazole donors bind to the so-called Cu_B (in C*c*Os) and Fe_B (in NORs). NORs are found in anaerobic denitrifiers which, instead of using dioxygen to pass electrons obtained from metabolic processes, use nitrogen oxides. The following biochemical pathway comes into play: $NO_3^{-} \rightarrow NO_2^{-} \rightarrow \bullet NO \rightarrow N_2O \rightarrow N_2$.[4,7] Each reaction step is catalyzed by metalloproteins.

*To whom correspondence should be addressed. E-mail: karlin@jhu.edu.

(1) Wang, J.; Schopfer, M. P.; Sarjeant, A. A. N.; Karlin, K. D. *J. Am. Chem. Soc.* **2009**, *131*, 450–451.
(2) Pinakoulaki, E.; Varotsis, C. *J. Inorg. Biochem.* **2008**, *102*, 1277–1287.
(3) Moënne-Loccoz, P. *Nat. Prod. Rep.* **2007**, *24*, 610–620.
(4) Wasser, I. M.; de Vries, S.; Moënne-Loccoz, P.; Schröder, I.; Karlin, K. D. *Chem. Rev.* **2002**, *102*, 1201–1234.
(5) Saraste, M.; Castresana, J. *FEBS Lett.* **1994**, *341*, 1–4.
(6) van der Oost, J.; de Boer, A. P. N.; de Gier, J.-W. L.; Zumft, W. G.; Stouthamer, A. H.; van Spanning, R. J. M. *FEMS Microbiol. Lett.* **1994**, *121*, 1–10.
(7) Averill, B. A. *Chem. Rev.* **1996**, *96*, 2951–2964.

Published on Web 12/23/2009

Scheme 1

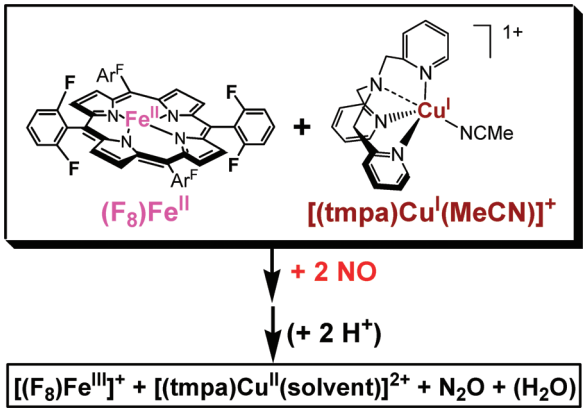

In the penultimate step in the mitrochondrial electron-transport chain, C*c*O's catalyze the four-electron reduction of dioxygen to water; this couples to inner-membrane proton translocation and a proton/charge gradient which powers the subsequent synthesis of ATP.[8−10] However, certain types of C*c*Os, such as ba_3 and caa_3 oxidases from *Thermus thermophilus*, cbb_3 oxidase from *Pseudomonas stutzeri*, and bo_3 from *Escherichia coli* also carry out nitrogen monoxide reductive coupling, that is, NOR chemistry,[11] and this subject has recently received considerable attention from the biophysical and computational research communities.[2,11−14] Lu and co-workers[15] have investigated such chemistry coming from a designed/modified small protein (myoglobin) model system. Here, a Cu_B center was designed and integrated into a wild-type myoglobin, leading to the formation of a protein with a binuclear heme/Cu center, which with an added external reductant was able to catalyze the $\bullet NO_{(g)}$ to N_2O conversion. Yet, we are far from having a sufficient understanding of the underlying metal/$\bullet NO_{(g)}$ and metal ion mediated NO−NO coupling chemistry.

In addition, the interaction of $\bullet NO_{(g)}$ with C*c*O's is of considerable importance.[16−22] Nitrogen monoxide reversibly inhibits mitochondrial respiration by binding to the C*c*O metal centers, influencing the regulation of mitochondrial reactive oxygen species generation and preventing cytochrome *c* release. There are also literature discussions concerning the reaction of $\bullet NO_{(g)}$ with C*c*O intermediates leading to its oxidation to nitrite;[23] this process may be biologically important for the purpose of generating pools of the latter, which may later be reduced back to NO (perhaps also by reduced C*c*O).[18,24] The interplay of •NO and O_2 chemistry at C*c*O metal centers and the control of relative levels of •NO (and nitrite) and O_2 (and rates of respiration) are biologically critical processes.

Thus, the reductive coupling of nitric oxide is of chemical and biological interest, and the study of systems undergoing this chemistry is part of our larger research program in the investigation of small molecule gases (O_2, NO, and CO) and their interactions with heme/M (M = Fe or Cu) binuclear assemblies.[1,10,25−27] As stated, here, we report on a system employing heme/Cu complexes, in fact, component heme and copper complexes along with the presence of acid, which function together to facilitate the stoichiometric $\bullet NO_{(g)}$ coupling reduction to $N_2O_{(g)}$, Scheme 1. As part of the description and chemistry involved, we describe the generation and some of the physical properties of a new complex, a heme dinitrosyl species $(F_8)Fe(NO)_2$. Also, the X-ray structure and spectroscopic characterization of a new heme−iron(III) complex, $[(F_8)Fe^{III}](SbF_6)$ (F_8 = tetrakis-(2,6-difluorophenyl)porphyrinate(2-)) are reported.

Experimental Section

Materials and Methods. Unless otherwise stated, all solvents and chemicals used were of commercially available analytical grade. Nitrogen monoxide (•NO) gas was obtained from Matheson Gases and passed multiple times through a column containing KOH pellets and through a liquid N_2 cooled trap to remove impurities (see also the Supporting Information of refs 27 & 28). The purified $\bullet NO_{(g)}$ was passed into a Schlenk flask placed in liquid N_2, to freeze. For use in reactions, this frozen gas was briefly warmed with the acetone/dry ice bath (−78 °C) and allowed to pass into an evacuated Schlenk flask (typically 50 mL) fitted with a septum. The addition of $\bullet NO_{(g)}$ to metal complex solutions was effected by transfer via a three-way long syringe needle. Dinitrogen oxide (N_2O) gas was purchased from Airgas as a custom mixture, at a concentration of 250 ppm, balanced with dinitrogen at 1 atm. Dichloromethane (CH_2Cl_2; DCM), acetonitrile (MeCN), methanol (MeOH), and pentane were used after passing through a 60-cm-long column of activated alumina (Innovative Technologies, Inc.) under argon. Tetrahydrofuran (THF) and acetone were purified and dried by distillation from sodium/benzophenone ketyl. Preparation and handling of air-sensitive compounds were performed under an argon atmosphere using standard Schlenk techniques or in an MBraun Labmaster 130 inert atmosphere (< 1 ppm O_2, < 1 ppm H_2O) drybox filled with nitrogen gas. Deoxygenation

(8) Ferguson-Miller, S.; Babcock, G. T. *Chem. Rev.* **1996**, *96*, 2889–2907.
(9) Collman, J. P.; Boulatov, R.; Sunderland, C. J.; Fu, L. *Chem. Rev.* **2004**, *104*, 561–588.
(10) Kim, E.; Chufán, E. E.; Kamaraj, K.; Karlin, K. D. *Chem. Rev.* **2004**, *104*, 1077–1133.
(11) Zumft, W. G. *J. Inorg. Biochem.* **2005**, *99*, 194–215.
(12) Hayashi, T.; Lin, M. T.; Ganesan, K.; Chen, Y.; Fee, J. A.; Gennis, R. B.; Moënne-Loccoz, P. *Biochemistry* **2009**, *48*, 883–890.
(13) Varotsis, C.; Ohta, T.; Kitagawa, T.; Soulimane, T.; Pinakoulaki, E. *Angew. Chem., Int. Ed.* **2007**, *46*, 2210–2214.
(14) Blomberg, L. M.; Blomberg, M. R. A.; Siegbahn, P. E. M. *Biochim. Biophys. Acta* **2006**, *1757*, 31–46.
(15) Zhao, X.; Yeung, N.; Russell, B. S.; Garner, D. K.; Lu, Y. *J. Am. Chem. Soc.* **2006**, *128*, 6766–6767.
(16) Cooper, C. E.; Brown, G. C. *J. Bioenerg. Biomembr.* **2008**, *40*, 533–539.
(17) Cooper, C. E.; Giulivi, C. *Am. J. Physiol. Cell Physiol.* **2007**, *292*, C1993–2003.
(18) Benamar, A.; Rolletschek, H.; Borisjuk, L.; Avelange-Macherel, M.-H.; Curien, G.; Mostefai, H. A.; Andriantsitohaina, R.; Macherel, D. *Biochim. Biophys. Acta* **2008**, *1777*, 1268–1275.
(19) Antunes, F.; Boveris, A.; Cadenas, E. *Antioxid. Redox Signaling* **2007**, *9*, 1569–1580.
(20) Mason, M. G.; Nicholls, P.; Wilson, M. T.; Cooper, C. E. *Proc. Natl. Acad. Sci. U.S.A.* **2006**, *103*, 708–713.
(21) Brunori, M.; Giuffre, A.; Forte, E.; Mastronicola, D.; Barone, M. C.; Sarti, P. *Biochim. Biophys. Acta* **2004**, *1655*, 365.
(22) Brudvig, G. W.; Stevens, T. H.; Chan, S. I. *Biochemistry* **1980**, *19*, 5275–5285.
(23) Cooper, C. E.; Mason, M. G.; Nicholls, P. *Biochim. Biophys. Acta* **2008**, *1777*, 867–876.
(24) Castello, P. R.; Woo, D. K.; Ball, K.; Wojcik, J.; Liu, L.; Poyton, R. O. *Proc. Natl. Acad. Sci. U.S.A.* **2008**, *105*, 8203–8208.
(25) Chufan, E. E.; Mondal, B.; Gandhi, T.; Kim, E.; Rubie, N. D.; Moenne-Loccoz, P.; Karlin, K. D. *Inorg. Chem.* **2007**, *46*, 6382–6394.
(26) Wasser, I. M.; Huang, H. W.; Moenne-Loccoz, P.; Karlin, K. D. *J. Am. Chem. Soc.* **2005**, *127*, 3310–3320.
(27) Schopfer, M. P.; Mondal, B.; Lee, D.-H.; Sarjeant, A. A. N.; Karlin, K. D. *J. Am. Chem. Soc.* **2009**, *131*, 11304–11305.
(28) Park, G. Y.; Deepalatha, S.; Puiu, S. C.; Lee, D.-H.; Mondal, B.; Narducci Sarjeant, A. A.; del Rio, D.; Pau, M. Y. M.; Solomon, E. I.; Karlin, K. D. *J. Biol. Inorg. Chem.* **2009**, *14*, 1301–1311.

of the solvents was effected by either repeated freeze/pump/thaw cycles or bubbling with argon for 30−45 min.

UV−vis spectra were recorded on a Hewlett-Packard Model 8453A diode array spectrophotometer equipped with a two-window quartz H.S. Martin Dewar filled with cold MeOH (+25 °C to −85 °C) maintained and controlled by a Neslab VLT-95 low-temperature circulator. Spectrophotometer cells used were made by Quark Glass with a column and pressure/vacuum side stopcock and 1 cm path length. Electron paramagnetic resonance (EPR) spectra were recorded on a Bruker EMX spectrometer controlled with a Bruker ER 041 X G microwave bridge operating at the X-band (~9.4 GHz). ESI mass spectra were acquired using a Finnigan LCQDeca ion-trap mass spectrometer equipped with an electrospray ionization source (Thermo Finnigan, San Jose, CA). The heated capillary temperature was 250 °C, and the spray voltage was 5 kV. Gas chromatography analysis was performed on a Varian CP-3800 instrument equipped with a 1041 manual injector, electron conductivity detector, and a 25 m 5 Å molecular sieve capillary column. Ion chromatography analysis (ICA) was performed on a Dionex DX-120 Ion chromatograph, with an AS40 automated sampler, and an IonPac AS14 (4*250 mm) column. The eluent was 3.5 mM Na_2CO_3 along with 1.0 mM $NaHCO_3$. See below for the procedure for generating a sample for ICA. Infrared spectra (IR) were recorded on a Bruker Vector 22 instrument controlled by OPUS-NT software at room temperature.

Low-Temperature NMR Spectroscopic Measurements. Multinuclear (^{1}H and ^{2}H) NMR spectroscopic measurements were performed at various temperatures under a N_2 atmosphere. ^{1}H NMR spectra were measured on a Bruker 400 MHz spectrometer, while ^{2}H NMR spectra were measured on a Varian Mercury 500 MHz spectrometer. Chemical shifts were reported as δ values relative to an internal standard of the deuterated solvent being used. Measurement of spectra for the mono- and dinitrosyl heme complexes was carried out in septum-capped NMR tubes, and $\bullet NO_{(g)}$ was added via an airtight syringe to −78 °C solutions.

X-Ray Structure Determination. X-ray diffraction was performed at the facility of the chemistry department of Johns Hopkins University. The X-ray intensity data were measured on an Oxford Diffraction Xcalibur3 system equipped with a graphite monochromator and an Enhance (Mo) X-ray Source (λ = 0.71073 Å) operated at 2 kW power (50 kV, 40 mA) and a CCD detector. The frames were integrated, scaled, and corrected for absorption using the Oxford Diffraction CrysAlisPRO software package.

Syntheses. $(F_8)FeCl$ (F_8 = tetrakis(2,6-difluorophenyl)porphyrinate(2-)),[29] $(F_8\text{-}d_8)FeCl$,[30] $(F_8)Fe^{II}$,[30] $(F_8\text{-}d_8)Fe^{II}$,[30] $(F_8)Fe(NO)$,[1] tris(2-pyridylmethyl)amine (TMPA),[31] $[(tmpa)Cu^I(MeCN)]PF_6$,[31] $[(tmpa)Cu^I(MeCN)]B(C_6F_5)_4$,[32] $[Cu^I(MeCN)_4]SbF_6$,[33] and $[H(C_2H_5OC_2H_5)_2][B(C_6F_5)_4]$ (HBArF)[34] were prepared from literature reports.

Synthesis of (THF)(F_8)Fe(NO). A solution of 75 mg (0.092 mmol) of $(F_8)Fe^{II}$ in 5 mL of THF was cooled to −78 °C using a dry ice/acetone bath. Under Ar, 20 mL of $\bullet NO_{(g)}$ at ~1 atm was added using a gastight syringe. The solution was stirred for 30 min, and degassed heptane was added until a solid product precipitated. The brown-red solid obtained (60 mg, 77%) was filtered and dried under a vacuum and then stored in the drybox. UV−vis (λ_{max}, nm): THF, 410 (Soret), 546. IR (cm^{-1}): ν_{NO} 1670 in THF. EPR spectrum, see Results and Discussion. Anal. Calcd for {(THF)(F_8)Fe(NO)·THF}, $C_{52}H_{36}F_8FeN_5O_3$: C, 63.30; H, 3.68; N, 7.10. Found: C, 62.76; H, 3.60; N, 6.94.

Synthesis of $[(F_8)Fe^{III}]SbF_6$. This synthesis is a modified version of that reported earlier for tetraphenylporphyrin.[35] In a glovebox filled with N_2, $(F_8)FeCl$ (0.30 g, 0.354 mmol) and $AgSbF_6$ (0.128 g, 0.373 mmol) were weighed and transferred to a Schlenk flask equipped with a stir bar. The solid materials were dissolved in 35 mL of freshly distilled THF, and the solution was stirred at room temperature for 1 h under reduced light. The reaction mixture was then filtered to remove AgCl. The filtrate was dried in vacuo, redissolved in 7 mL of CH_2Cl_2, and precipitated twice with the addition of 80 mL of pentane, yielding a purple powder (250 mg, 83%). UV−vis (λ_{max}, nm): CH_2Cl_2, 328, 394 (Soret), 512; THF, 328, 394 (Soret), 510. IR (Nujol, cm^{-1}): ν_{SbF6} 657 cm^{-1}. EPR spectrum at 77 K: g = 5.84 (in DCM); g = 6.12 (in THF). ESI-MS: 812.5, $(F_8)Fe$. ^{1}H NMR (CD_2Cl_2): δ 27.2 and 11.6 (8 pyrrole), 10.2 (4 para), 9.4 (8 meta). ^{1}H NMR (THF-d_8): δ 54.7 and 14.8 (8 pyrrole), 10.4 (4 para), 9.3 (8 meta). Anal. Calcd for $\{(F_8)FeSbF_6\cdot 1.5CH_2Cl_2\}$, $C_{45.5}H_{23}Cl_3F_{14}FeN_4Sb$: C, 46.48; H, 1.97; N, 4.75. Found: C, 46.38; H, 2.12; N, 4.66. Crystals, suitable for X-ray diffraction, were obtained by layering a concentrated tetrahyrdrofuran solution of $[(F_8)Fe^{III}]SbF_6$ with pentane. The purple-colored X-ray-quality crystals are formulated as $[(F_8)Fe^{III}(THF)_2]SbF_6$. See the Results and Discussion for further information.

Synthesis of $[(tmpa)Cu^{II}(MeCN)](ClO_4)_2$. TMPA (1.51 g, 5.20 mmol) and $Cu(ClO_4)_2\cdot 6H_2O$ (1.93 g, 5.21 mmol) were dissolved in a total of 40 mL of CH_3CN and allowed to stir for 30 min, whereupon a dark blue solution developed. Diethyl ether (90 mL) was added to give a crude precipitate. Recrystallization of this solid from CH_3CN/ether and drying in vacuo gave a light blue powder in a yield of 86% (2.66 g). Anal. Calcd for $[(tmpa)Cu^{II}(MeCN)](ClO_4)_2$, $C_{20}H_{21}Cl_2CuN_5O_8$: C, 40.45; H, 3.56; N, 11.79. Found: C, 40.55; H, 3.53; N, 11.80. UV−vis (CH_3CN, λ_{max}, nm (ε, $M^{-1}\,cm^{-1}$)): 255 (14 700), 855 (254). EPR spectrum in acetone at 77 K (see Figure S1, Supporting Information): $g_\perp$ = 2.22, $g_\parallel$ = 2.02, $A_\perp$ = 105 G, $A_\parallel$ = 71 G.

Synthesis of $[(tmpa)Cu^{II}(NO_2)]PF_6$. To a 100 mL Schlenk flask equipped with a magnetic stir bar was added 200 mg of $[(tmpa)Cu^I(MeCN)]PF_6$ in degassed CH_3CN/THF (50:50) under a N_2 atmosphere. The reaction flask was incubated in an acetone/dry ice bath. Excess $\bullet NO_{(g)}$ was bubbled through this solution, and the reaction mixture was allowed to stir for 30 min, with the color turning from yellow to purple. The solution was warmed to room temperature (RT), with its color turning to green, and this was kept stirring for 2 h. Solvents were removed under reduced pressure, and then recrystallization of the green solid from CH_3CN/ether gave a green microcrystalline solid (75%). IR (in DCM, cm^{-1}): ν_{as} (NO_2) 1390, ν_{as} (NO_2) 1330. UV−vis (λ_{max}, nm, in CH_2Cl_2): 301, 415 (see Figure S2, Supporting Information). EPR spectrum in acetone at 77 K (see Figure S3, Supporting Information): $g_\perp$ = 2.21, $g_\parallel$ = 2.01, $A_\perp$ = 84 G, $A_\parallel$ = 80 G. Anal. Calcd for $[(tmpa)Cu^{II}(NO_2)]PF_6$, $C_{18}H_{18}CuF_6N_5O_2P$: C, 39.68; H, 3.33; N, 12.85. Found: C, 39.76; H, 3.50; N, 12.27. Nitrite (NO_2^-) was the only detectable ion in the green solid, as determined using ICA. See below for the procedure for generating a sample for ICA.

Synthesis of $[(tmpa)Cu^I(MeCN)]SbF_6$. This synthesis followed a procedure similar to that reported earlier for $[(tmpa)Cu^I(MeCN)_4]PF_6$.[31] A solution of 200 mg (0.689 mmol) of TMPA ligand in 10 mL of distilled CH_3CN was added to

(29) Karlin, K. D.; Nanthakumar, A.; Fox, S.; Murthy, N. N.; Ravi, N.; Huynh, B. H.; Orosz, R. D.; Day, E. P. *J. Am. Chem. Soc.* **1994**, *116*, 4753–4763.

(30) Ghiladi, R. A.; Kretzer, R. M.; Guzei, I.; Rheingold, A. L.; Neuhold, Y.-M.; Hatwell, K. R.; Zuberbühler, A. D.; Karlin, K. D. *Inorg. Chem.* **2001**, *40*, 5754–5767.

(31) Tyeklár, Z.; Jacobson, R. R.; Wei, N.; Murthy, N. N.; Zubieta, J.; Karlin, K. D. *J. Am. Chem. Soc.* **1993**, *115*, 2677–2689.

(32) Zhang, C. X.; Liang, H.-C.; Kim, E.-i.; Shearer, J.; Helton, M. E.; Kim, E.; Kaderli, S.; Incarvito, C. D.; Zuberbühler, A. D.; Rheingold, A. L.; Karlin, K. D. *J. Am. Chem. Soc.* **2003**, *125*, 634–635.

(33) Kubas, G. J. *Inorg. Synth.* **1990**, *28*, 68–70.

(34) Jutzi, P.; Muller, C.; Stammler, A.; Stammler, H. G. *Organometallics* **2000**, *19*, 1442–1444.

(35) Reed, C. A.; Mashiko, T.; Bentley, S. P.; Kastner, M. E.; Scheidt, W. R.; Spartalian, K.; Lang, G. *J. Am. Chem. Soc.* **1979**, *101*, 2948–2958.

319 mg (0.689 mmol) of $[Cu(CH_3CN)_4]SbF_6$ in a 100 mL Schlenk flask in the glovebox; the solution was stirred for 1 h. Afterward, 75 mL of diethyl ether was added to the bright orange solution until a slight cloudiness was observed to develop. The solution was filtered through a medium-porosity frit, and the compound obtained was recrystallized from CH_3CN/ether. The precipitate formed was dried under vacuum, leading to a yellow-orange solid (78%). ^{1}H NMR (CD_3CN): δ 8.93 (br, 3H), 7.83 (m, 3 H), 7.50 (br, 6 H), 4.3 (v br, 6 H), 2.01 (s, 3 H, CH_3CN).

Synthesis of [(tmpa)Cu^{II}(NO$_2$)]SbF$_6$. To a 100 mL Schlenk flask equipped with a magnetic stir bar was added 300 mg of $[(tmpa)Cu^{I}(MeCN)]SbF_6$ in degassed CH_3CN/THF (50:50) under a N_2 atmosphere. The reaction flask was then incubated in an acetone/dry ice bath and the solution bubbled with excess $NO_{(g)}$. The reaction mixture was allowed to stir for 30 min with the color turning from yellow to purple. Subsequently, the closed system warmed to RT, now turning to green, and this solution was stirred at RT for 2 h. Solvents were removed under reduced pressure, and recrystallization of the resulting solid from CH_3CN/ether gave a green microcrystalline solid $[(tmpa)Cu^{II}(NO_2)]SbF_6$ (70% yield). IR (in CH_2Cl_2, cm^{-1}): $\nu_{as}(NO_2)$ 1390, ν_{as} (NO_2) 1330. Anal. Calcd for $[(tmpa)Cu^{II}(NO_2)]SbF_6$, $C_{18}H_{18}CuF_6N_5O_2Sb$: C, 34.01; H, 2.85; N, 11.02. Found: C, 33.72; H, 2.80; N, 10.58. UV−vis (λ_{max}, nm, in CH_2Cl_2): 301, 415. Nitrite (NO_2^-) was the only ion detected following ion chromatography analysis on this green solid. See below for the procedure for generating a sample for ICA.

Generation of (F$_8$)Fe(NO)$_2$. A 5 mL distilled acetone solution of $(F_8)Fe(NO)$ (5×10^{-6} mol/L) was taken in a UV−vis cuvette assembly under argon; it was cooled to −78 °C, and an initial spectrum was recorded. Excess $\bullet NO_{(g)}$ was bubbled through the cold solution using a three-way needle syringe, and the new spectrum (of $(F_8)Fe(NO)_2$) was recorded, λ_{max} = 426 (Soret), 538 nm. Additional bubbling with $\bullet NO_{(g)}$ did not change the spectrum further. This resulting species $(F_8)Fe(NO)_2$ released NO to form $(F_8)Fe(NO)$ upon warming to RT, and $(F_8)Fe(NO)_2$ was regenerated when cooling to −80 °C or adding more $NO_{(g)}$. The other protocol for $(F_8)Fe(NO)_2$ generation was bubbling excess $\bullet NO_{(g)}$ into the reduced complex $(F_8)Fe^{II}$ at −80 °C, while $(F_8)FeNO$ was formed if $\bullet NO_{(g)}$ reacted with $(F_8)Fe^{II}$ at RT. ^{1}H NMR (CD_2Cl_2): δ 9.13 and 8.93 (8 pyrrole), 7.84 (4 para), 7.45 (8 meta). EPR spectrum in acetone at 77 K: silent. The related deuterated complex, $(F_8$-$d_8)Fe(NO)_2$, was generated in a similar manner, except starting with $(F_8$-$d_8)Fe(NO)$. $(F_8$-$d_8)Fe(NO)$ was synthesized from $(F_8$-$d_8)Fe^{II}$ nitrosylation by bubbling $\bullet NO_{(g)}$ through the $(F_8$-$d_8)Fe^{II}$ solution (in CH_2Cl_2) and removal of excess $\bullet NO_{(g)}$ and solvents to yield a purple solid.

Titration of (F$_8$)Fe(NO)$_2$ with (F$_8$)Fe^{II}. $(F_8)Fe^{II}$ (0.0019 g, 0.0023 mmol) was dissolved in 100 mL of deaerated THF inside the glovebox. From the red solution, 10 mL was transferred into a Schlenk flask, and under an Ar atmosphere on the benchtop this was cooled to −78 °C and a spectrum recorded {λ_{max} = 422 (Soret), 542 nm}. Afterward, excess $\bullet NO_{(g)}$ was bubbled through this cold solution using a three-way long needle syringe, the resulting new spectrum of the orange product $(F_8)Fe(NO)_2$ was recorded, {λ_{max} = 410 (Soret), 540 nm}. Additional bubbling with $\bullet NO_{(g)}$ did not change the spectrum further. The cold mixture was then purged with an Ar flow for 1 min, and the entire flask was evacuated and refilled with Ar three times to remove the excess $\bullet NO_{(g)}$. There was no spectral change upon excess $\bullet NO_{(g)}$ removal. Approximately 1 equiv of $(F_8)Fe^{II}$ was added to the cold solution by transferring 10 mL of the cold (−78 °C) $(F_8)Fe^{II}$ stock solution in THF with a cannula technique. At −78 °C, the spectrum indicated it was a mixture of mononitrosyl, dinitrosyl, and $(F_8)Fe^{II}$. However, upon warming to RT, only one product was present, $(THF)(F_8)Fe(NO)$, {λ_{max} = 410 (Soret), 546 nm} (see Figure S4, Supporting Information). On the basis of the known extinction coefficients for $(THF)(F_8)Fe(NO)$ {λ_{max} = 410 nm (Soret), ε = 176 000 M^{-1} cm^{-1}; 546 nm, ε = 8300 M^{-1} cm^{-1}}, the mononitrosyl species was formed in approximately 90% yield on the basis of the reaction, $(F_8)Fe(NO)_2 + (F_8)Fe^{II} \rightarrow 2(THF)(F_8)Fe(NO)$ (in THF solution).

Reaction of (F$_8$)Fe(NO)$_2$ with [(tmpa)Cu(MeCN)]PF$_6$ and Acid. Complex $(F_8)Fe(NO)$ (0.050 g, 0.059 mmol) was dissolved in 10 mL of distilled acetone in a 50 mL Schlenk flask and then cooled to −78 °C using an acetone/dry ice bath. Excess $\bullet NO_{(g)}$ was bubbled through the orange cold solution using a three-way syringe, and then the excess $\bullet NO_{(g)}$ was removed via vacuum/purge cycles. After stirring for 30 min, the orange solution was added to the prechilled $[(tmpa)Cu^{I}(MeCN)][B(C_6F_5)_4]$ in 10 mL of an acetone/MeCN (1:1; 0.064 mg, 0.060 mmol) solution via a two-way syringe needle. After stirring for 10 min, a 5 mL acetonitrile solution of $[H(C_2H_5OC_2H_5)_2][B(C_6F_5)_4]$ (HBArF) (0.098 mg, 0.118 mmol) was added to the cold orange solution mixture. It turned to brown upon warming to RT. The solution was concentrated in vacuo, and addition of deoxygenated pentane led to a brown solid. UV−vis (λ_{max}, nm): CH_2Cl_2, 394 (Soret), 512; THF, 394 (Soret), 511. IR (Nujol, cm^{-1}): no related ν_{NO} observed. EPR spectrum in acetone (77 K): g = 6.12 (heme−Fe^{III}); $g_\perp$ = 2.21, $g_\parallel$ = 2.01, $A_\perp$ = 100 G, $A_\parallel$ = 68 G (Cu^{II}). ESI-MS in MeCN: (813, (F_8)-Fe + H; 853, $(F_8)Fe$ + MeCN; 871, $(F_8)Fe + H_2O$ + MeCN; 353, (tmpa)Cu). A 10 mL CH_2Cl_2 solution of the brown solid product was mixed with 10 mL of aqueous NaCl solution (400 uM) and stirred for half an hour. Ion chromatography analysis of this upper aqueous layer extract gave no indication for the presence of any nitrite ion (NO_2^-).

Gas chromatography analysis of the head space of this reaction mixture reveals $N_2O_{(g)}$ formed in a yield of 84% according to the stoichiometry $2\bullet NO + 2\,e^- + 2\,H^+ \rightarrow N_2O_{(g)} + H_2O$. Thus, the metal complex products of the reaction are $[(F_8)Fe^{III}]^+$ and $[(tmpa)Cu^{II}(solvent)]^{2+}$, along with $N_2O_{(g)}$. See the Results and Discussion for further information or clarification.

Reaction of (F$_8$)Fe(NO)$_2$ with [(tmpa)Cu(MeCN)]PF$_6$. Complex $(F_8)Fe(NO)$ (0.040 g, 0.047 mmol) was dissolved in 10 mL of distilled acetone and then cooled to −78 °C using an acetone/dry ice bath. Excess $\bullet NO_{(g)}$ was bubbled through the cold solution using a three-way syringe. After stirring for 30 min, the orange solution of $(F_8)Fe(NO)_2$ was added to a precooled $[(tmpa)Cu^{I}(MeCN)]PF_6$ (0.026 mg, 0.048 mmol) solution in 10 mL of acetone/MeCN (1:1) via a two-way syringe needle, and the mixture was allowed to stir for 30 min. After warming to RT, the solution mixture kept stirring for 1 h and then was concentrated in a vacuum. The addition of 70 mL of deoxygenated pentane precipitated the orange product solution as a mixture of purple and green solids. An EPR spectrum indicated that the product was a mixture of $(F_8)Fe(NO)$ and Cu^{II} species, while an IR spectrum of this solid (Nujol mull) indicated that one $\bullet NO$ molecule is still bound to the $(F_8)Fe$ fragment, ν_{NO} = 1684 cm^{-1}. UV−vis (λ_{max}, nm): THF, 410 (Soret), 546; CH_2Cl_2, 400 (Soret), 540. To determine what other nitrogen oxide products formed, a series of stock solutions of synthetically derived $[(tmpa)Cu(NO_2)]SbF_6$ (vide supra) were generated, mixing (30 min) 10 mL of CH_2Cl_2 with 10 mL of aqueous NaCl (160 μM). The upper aqueous layer extract was taken for nitrite ion analysis on the Dionex DX-120 Ion chromatograph (see above for the procedure for generating a sample for ICA), and then a calibration curved was formed. Afterward, the product mixture of the reaction of 20 mg $(F_8)Fe(NO)_2$ + 13 mg $[(tmpa)Cu^{I}(MeCN)]PF_6$ (1:1 molar ratio) was analyzed for ion fractions via the same method. Via this nitrite analysis, $[(tmpa)Cu(NO_2)]PF_6$ was found to form in a yield of 95%, on the basis of the reaction stoichiometry: $3\bullet NO + [(L)Cu^{I}]^+ \rightarrow N_2O + [(L)Cu^{II}(NO_2^-)]^+$. Thus, the metal complex products of

Scheme 2

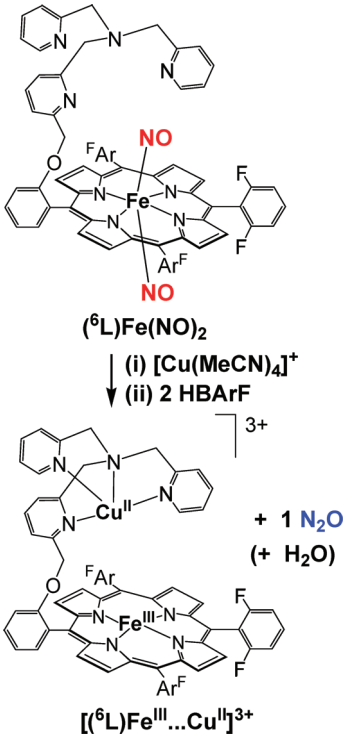

the reaction are $(F_8)Fe(NO)$ plus a mixture of 1/3[(tmpa)Cu^{II}-(NO_2)]PF_6 and unreacted 2/3[(tmpa)Cu^{I}(solvent)]$^+$. Gas chromatography analysis of the head space of the original reaction mixture reveals $N_2O_{(g)}$ formed in a yield of 88% according to this stoichiometry. See the Results and Discussion for further information or clarification.

Results and Discussion

We previously reported on $\bullet NO_{(g)}$ reductive coupling chemistry carried out by a binuclear heme/Cu assembly with a binucleating ligand referred to as ^{6}L; with the formation of a heme−dinitrosyl complex (^{6}L)$Fe(NO)_2$, the addition of a copper(I) ion source along with acid led to excellent yields of $N_2O_{(g)}$ (Scheme 2).[1] In that study, the use of a heterobinucleating ligand made sense in terms of a synthetic strategy in carrying out such cooperative heme/Cu/small-molecule investigations. This would vastly increase the liklihood that this reductive coupling chemistry was not resulting from heme−heme or copper−copper reactions.

In fact, the use of component mixtures of heme and separate copper complexes has been previously very successful for our study of heme/Cu/O_2 reactivity, leading to the generation and characterization of quite a large series of heme/Cu/O_2 adducts, including those with ^{6}L.[10,25,36,37] Thus, here we chose to also apply that approach with respect to $\bullet NO_{(g)}$ reductive coupling chemistry, thus hopefully effected by a distinct heme together with a copper complex. Scheme 3 summarizes the chemical transformations described in this paper and depicts all of the important individual complexes which have been characterized and will be discussed in this report.

As shown in Scheme 3, the mononitrosyl complex $(F_8)Fe(NO)$ reacted with $\bullet NO_{(g)}$ to form the dinitrosyl species, $(F_8)Fe(NO)_2$, very similar in properties to the dinitrosyl complex generated in situ in the ^{6}L system, (^{6}L)$Fe(NO)_2$ (Scheme 2).[1] Once discovering that such complexes exist and can be generated in a stoichiometric manner (vida infra), we wished to take advantage of this fact that *exactly* two •NO molecules are present for each heme or heme/Cu assembly. This would, as it turns out for the ^{6}L binucleating system and also here, allow for a stoichiometric reaction, for example, one synthetic model enzyme turnover:

$$2\bullet NO + Fe^{II} + Cu^{I} + 2H^{+} \rightarrow N_2O_{(g)} + Fe^{III} + Cu^{II} + H_2O \quad (1)$$

Exactly this reaction occurs when $(F_8)Fe(NO)_2$ is added to [(tmpa)Cu^{I}(MeCN)]$^+$ in the presence of 2 equiv of acid, the latter in the form of $H(Et_2O)_2[B(C_6F_5)_4]$. The NOR type reaction occurs and the particular products obtained are $[(F_8)Fe^{III}]^+$, [(tmpa)Cu^{II}(solvent)]$^{2+}$, and $N_2O_{(g)}$. However, when acid is absent, the reaction of $(F_8)Fe(NO)_2$ and [(tmpa)Cu^{I}(MeCN)]$^+$ yields different products, and different $\bullet NO_{(g)}$/metal chemistry takes place (Scheme 3). Details are provided in the subsequent sections.

Mononitrosyl Complexes $(F_8)Fe(NO)$ and (THF)-$(F_8)Fe(NO)$. We recently[1] reported on the synthesis and X-ray structure of $(F_8)Fe(NO)$, that formed via the reductive nitrosylation of $(F_8)Fe^{III}Cl$. It can also be generated by bubbling $\bullet NO_{(g)}$ through a $(F_8)Fe^{II}$ solution, that is, $(F_8)Fe^{II}$ + NO → $(F_8)Fe(NO)$ (see the Experimental Section). $(F_8)Fe(NO)$ is a stable complex as a solid and in solution, and unreactive toward dioxygen. It displays a N−O stretching frequency at 1684 cm^{-1} (Nujol), 1691 cm^{-1} in CH_2Cl_2 solution, and 1670 cm^{-1} in THF. It gives the expected classic rhombic EPR spectrum with three-line hyperfine splitting pattern due to unpaired electron interaction with ^{14}N (I = 1) of the nitrosyl ligand (g_1 = 2.113, g_2 = 2.078, g_3 = 2.025), Figure 1.

In the course of our studies with heme/Cu/O_2 reactivity using $(F_8)Fe^{II}$, we have explored the use of various solvents and found, for example, that acetone, THF, and RCN (R = Me, Et) solvents bind the heme as axial "base" ligands.[30] THF is particularly strong compared to the others. In fact, THF is found to bind quite strongly to $(F_8)Fe(NO)$, affording $(THF)(F_8)Fe(NO)$. We were able to isolate this six-coordinate nitrosyl complex, the first with an oxygen donor to be characterized by elemental analysis, IR, EPR, and UV−vis spectroscopies. In Table 1, we compare IR, EPR, and UV−vis parameters for $(THF)(F_8)Fe(NO)$, $(F_8)Fe(NO)$, various other (porphyrinate)Fe(NO) complexes, and a previously described bis-THF adduct, $(THF)_2Fe^{II}$.[38] Figure 2 shows the EPR spectrum of $(THF)(F_8)Fe(NO)$ recorded at 77 K in THF.

The subfield of heme−nitrosyl complexes, synthetic or biological, is already very mature, although it continues

(36) Chufán, E. E.; Puiu, S. C.; Karlin, K. D. *Acc. Chem. Res.* **2007**, *40*, 563–572.
(37) Ghiladi, R. A.; Ju, T. D.; Lee, D.-H.; Moënne-Loccoz, P.; Kaderli, S.; Neuhold, Y.-M.; Zuberbühler, A. D.; Woods, A. S.; Cotter, R. J.; Karlin, K. D. *J. Am. Chem. Soc.* **1999**, *121*, 9885–9886.
(38) Thompson, D. W.; Kretzer, R. M.; Lebeau, E. L.; Scaltrito, D. V.; Ghiladi, R. A.; Lam, K.-C.; Rheingold, A. L.; Karlin, K. D.; Meyer, G. J. *Inorg. Chem.* **2003**, *42*, 5211–5218.
(39) Wyllie, G. R. A.; Scheidt, W. R. *Chem. Rev.* **2002**, *102*, 1067–1089.

Scheme 3

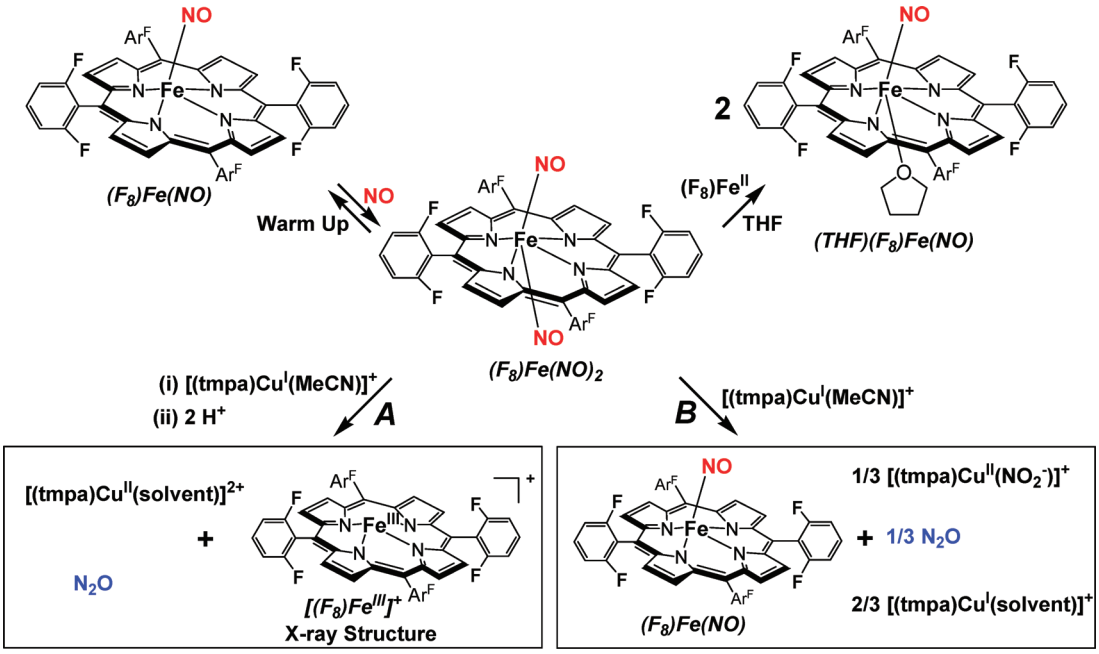

to draw considerable interest, due to more recently described biological processes which utilize or process •NO and its oxidized and reduced derivatives. There are many spectroscopically and structurally characterized five-coordinate and six-coordinate heme−nitrosyl complexes, so-called $\{FeNO\}^7$ derivatives, the value of seven derived from the six d electrons (i.e., $3d^6$) of iron(II) plus the unpaired electron from •NO.[44,45] It seems to be the case that there are only quite small differences in structural coordination parameters comparing complexes with different coordination numbers. However, IR spectra clearly suggest that, with an axial "base" binding to a trans/sixth position of a heme−NO moiety, the N−O stretching frequency shifts to a lower value.[46] For example, (TPP)Fe(NO) has a N−O stretch at 1670 cm^{-1}, which shifts to 1653 and 1625 when 4-methylpiperidine (4-MePip) and 1-methylimidazole (1-MeIm) are axially bound, respectively (Table 1). In the case of (F_8)Fe(NO) ($\nu_{(N-O)}$ = 1684 cm^{-1}), $\nu_{(N-O)}$ decreases by only 15 cm^{-1} with THF binding, but by 60 cm^{-1} with 1-MeIm binding.[40] Thus, our data clearly show that THF is a significant base, but much weaker than N-donor ligands such as 1-methylimidazole, which has been reported[40] to effect a much larger (60 cm^{-1}) shift to lower frequency.

Another difference between five- and six-coordinated heme−NO species is their EPR spectroscopic behavior. Five-coordinated complexes always exhibit the triplet hyperfine as described above for (F_8)Fe(NO).[41,47] Depending on the sixth axial trans ligand, (L)(porpyrinate)Fe(NO) complexes reveal two different types of hyperfine splitting patterns. Most possess a nine-line pattern localized to the g_2 or g_3 region,[41,48] due to the N hyperfine spitting of both the trans-*N* ligand and •NO; that is, a triplet of triplets is observed. There are only a few six-coordinate complexes with *O*-donor trans ligands.[41,42] (THF)(PPDME)Fe(NO) shows a three-line spectrum, but with smaller *g* values than that of five-coordinated(PPDME)Fe(NO) (Table 1). It was suggested that this indicates electronic interaction of THF occurs though the lone pair electrons on the oxygen atom. Of course, this conclusion is readily observed from IR spectroscopic data on our own (THF)(F_8)Fe(NO) complex (vide supra). Also, an EPR spectrum of this complex is nearly identical to that observed for (THF)(PPDME)Fe(NO), with a three-line pattern with *g* values (g_1 = 2.100, g_2 = 2.063, g_3 = 2.011) altered somewhat from that seen for (F_8)Fe(NO), see Figure 2 and Table 1.

Dinitrosyl Complex (F_8)Fe$(NO)_2$. This complex can be generated by bubbling excess $\bullet NO_{(g)}$ through solutions of either (a) the $(F_8)Fe^{II}$ reduced compound or (b) the mononitrosyl complex (F_8)Fe(NO) (see the Experimental Section). For purposes of characterization and reactivity studies, excess $\bullet NO_{(g)}$ was removed by the application of vacuum/purge cycles. An EPR spectrum of such a sample of $(F_8)Fe(NO)_2$ in acetone (77 K) shows the compound to be EPR-silent (Figure 1). This is consistent with it being diamagnetic, as might be expected by its formation from

(40) Praneeth, V. K. K.; Nather, C.; Peters, G.; Lehnert, N. *Inorg. Chem.* **2006**, *45*, 2795–2811.
(41) Cheng, L.; Richter-Addo, G. B. Binding and Activation of Nitric Oxide by Metalloporphyrins and Heme. In *Porphyrin Handbook*; Kadish, K. M., Simith, K. M., Guilard, R., Eds.; Academic Press: San Diego, CA, 2000; Vol. *4*, Chapter 33, pp 219−291.
(42) Yoshimura, T. *Inorg. Chim. Acta* **1982**, *57*, 99–105.
(43) Lorkovic, I.; Ford, P. C. *J. Am. Chem. Soc.* **2000**, *122*, 6516–6517.
(44) Enemark, J. H.; Feltham, R. D. *Coord. Chem. Rev.* **1974**, *13*, 339–406.
(45) Lee, D.-H.; Mondal, B.; Karlin, K. D. NO and N_2O Binding and Reduction. In *Activation of Small Molecules: Organometallic and Bioinorganic Perspectives*; Tolman, W. B., Ed.; Wiley-VCH: New York, 2006; pp 43−79.
(46) As is well understood, the sixth ligand provides additional electron density to the iron ion, which leads to enhanced backbonding to the π^*(NO) orbital, thus weakening the N−O bond and lowering ν(N−O).
(47) Ford, P. C.; Lorkovic, I. M. *Chem. Rev.* **2002**, *102*, 993–1017.
(48) Walker, F. A.; Simonis, U. Iron Porphyrin Chemistry. In *Encyclopedia of Inorganic Chemistry*, 2nd ed.; King, R. B., Ed.; John Wiley & Sons Ltd.: New York, 2005; Vol. *IV*; pp 2390−2521.

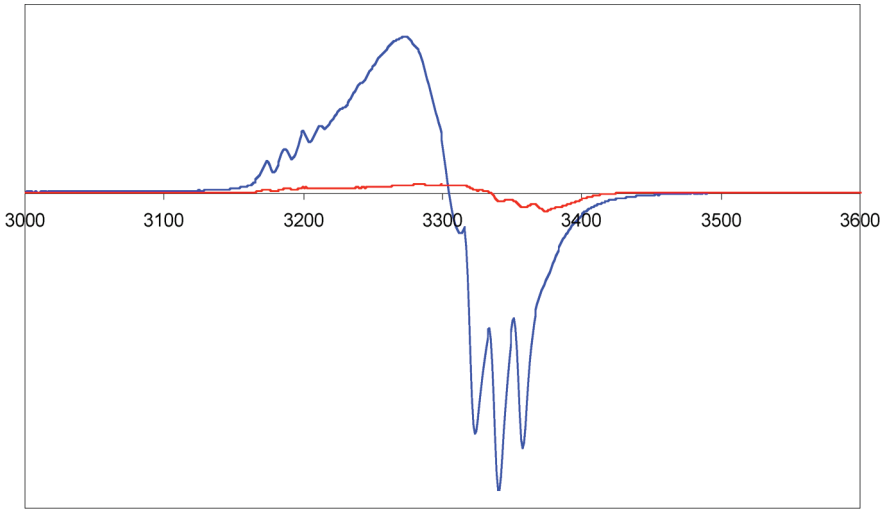

Figure 1. EPR spectra of $(F_8)Fe(NO)_2$ (red) and $(F_8)FeNO$ (blue) at the same concentration in acetone, recorded at 77 K.

Table 1. Comparisons of Structural Parameters for Heme Nitrosyl and Related Complexes[a]

complex	ν_{NO} (solvent), cm^{-1}	λ_{max} (nm)	g value	ref
		Five-Coordinate		
(TPP)Fe(NO)	1670 (KBr), 1678 (CH_2Cl_2)	405 (Soret), 537, 606 ($CHCl_3$)	$g_1 = 2.102$, $g_2 = 2.064$, $g_3 = 2.010$	39
($TPPBr_8$)Fe(NO)	1685 (KBr)			39
(T2,6-Cl_2PP)Fe(NO)	1688 (KBr)			39
(F_8)Fe(NO)	1684 (Nujol), 1691 (CH_2Cl_2)	400 (Soret), 541 (CH_2Cl_2)	$g_1 = 2.113$, $g_2 = 2.078$, $g_3 = 2.025$	this work
		Six-Coordinate		
(1-MeIm)(TPP)Fe(NO)	1625 (KBr)			39
(4-MePip)(TPP)Fe(NO)	1653 (KBr)			39
(1-MeIm)(F_8)Fe(NO)	1624 (KBr)			40
(THF)(PPDME)Fe(NO)			$g_1 = 2.096$, $g_2 = 2.050$, $g_3 = 2.011$	41, 42
(THF)(F_8)Fe(NO)	1669 (THF); 1684 (weak; due to (F_8)Fe(NO))	410 (Soret), 546 (THF)	$g_1 = 2.100$, $g_2 = 2.063$, $g_3 = 2.011$	this work
$(THF)_2(F_8)Fe$		422 (Soret), 544 (THF)	silent	38
$(F_8)Fe(NO)_2$		426 (Soret), 538 (acetone)	silent	this work
$(TmTP)Fe(NO)_2$	1696 (methylcyclohexane)	416 (Soret), 540 (methylcyclohexane)		43
$(TPP)Fe(NO)_2$	1695 ($CHCl_3$)			43

[a] Abbreviations used: TPP = *meso*-tetraphenylporphyrin; $TPPBr_8$ = octabromo-tetraphenylporphyrin; T2,6-Cl_2PP = 2,6-difluorophenylporphyrin; 1-MeIm = 1-methylimidazole; 4-MePip = 4-methylpiperidine; PPDME = protoporphyrin IX dimethyl ester; TmTP = *meso*-tetra-*m*-tolyl-porphinato dianion.

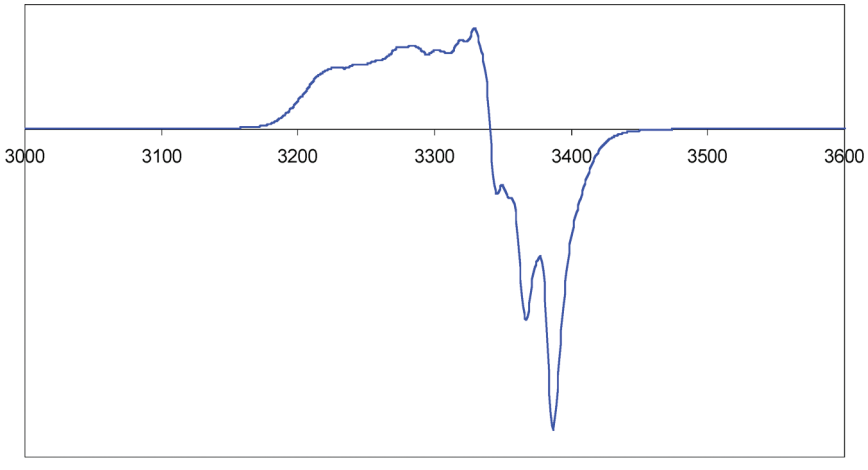

Figure 2. EPR spectrum of (THF)(F_8)Fe(NO) recorded at 77 K in THF with $g_1 = 2.100$, $g_2 = 2.063$, and $g_3 = 2.011$. It is essentially identical to the spectrum of (THF)(PPDME)Fe(NO), reported by Yoshimura.[42]

the radical species (F_8)Fe(NO) ($S = 1/2$) by the addition of another radical, •NO. As discussed below, NMR spectroscopic data are also consistent with the diamagnetism of $(F_8)Fe(NO)_2$.

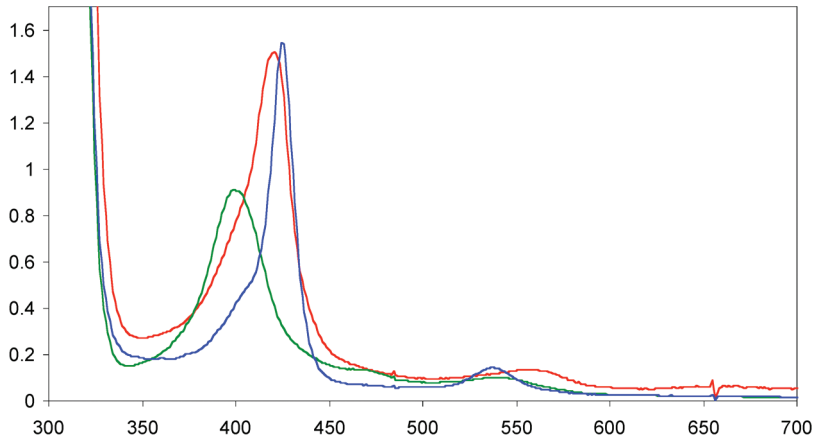

Figure 3. UV−vis spectrum of $(F_8)Fe(NO)_2$ (blue, λ_{max} = 426 (Soret), 538 nm) generated from $(F_8)Fe^{II}$ (red, λ_{max} = 421 (Soret), 553 nm) in acetone at −80 °C. Upon warming the solution (in a closed cuvette glassware apparatus), the mononitrosyl species $(F_8)Fe(NO)$ reforms (green, λ_{max} = 399 (Soret), 540 nm).

$$(F_8)Fe(NO) \underset{\text{warm up}}{\overset{+NO}{\rightleftharpoons}} (F_8)Fe(NO)_2 \qquad (2)$$

In fact, the binding of $\bullet NO_{(g)}$ to $(F_8)Fe(NO)$ is reversible, as can be monitored by EPR and UV−vis spectroscopies. Warming of an EPR sample of $(F_8)Fe(NO)_2$, removing gases in vacuo, and refreezing and now recording an EPR spectrum leads to regeneration of most of the triplet EPR spectrum due to $(F_8)Fe(NO)$. A UV−vis spectrum of $(F_8)Fe(NO)$ shows absorptions at 399 (Soret) and 541 nm in acetone, which change when excess $NO_{(g)}$ is bubbled through the cold solution, forming $(F_8)Fe(NO)_2$ (Figure 3). There is no obvious color change of the reaction solution in either solvent. When $(F_8)Fe(NO)_2$ is warmed to RT, whether excess $\bullet NO_{(g)}$ is present or not, $(F_8)Fe(NO)$ is reformed (eq 2).

To further confirm the formulation of the dinitrosyl complex $(F_8)Fe(NO)_2$, we added 1 equiv of the reduced compound $(F_8)Fe^{II}$ to a low-temperature solution of $(F_8)Fe(NO)_2$ from which excess $\bullet NO_{(g)}$ had been removed via vacuum/purge cycles. There is some immediate transfer to give a mixture of mono- and dinitrosyl complexes, based on UV−vis spectroscopy (Figure S4, Supporting Information). However, warming to RT results in the full formation of 2 equiv of $(F_8)Fe(NO)$; thus, the overall reaction proceeded as follows: $(F_8)Fe(NO)_2 + (F_8)Fe^{II} \rightarrow 2\ (F_8)Fe(NO)$. Not only does this experiment demonstrate that our low-temperature species is a dinitrosyl complex, that is, possessing two NO molecules per iron, but that the second NO molecule binds much more weakly than the first and can be extracted by another heme molecule.

NMR Spectroscopy for the Heme−Nitrosyl Complexes. At RT, a ^1H NMR spectrum of $(F_8)Fe(NO)$ gives a broad pyrrole proton signal at 6.05 ppm (Table 2), consistent with that found for other heme mononitrosyl compounds (Table 2).[40] Rather interesting temperature-dependent behavior occurs, as is now described along with tentative interpretations. As shown in Figure 4 and Figure S5 (Supporting Information), ^1H NMR spectra of $(F_8)Fe(NO)$ were recorded at +20 °C, −20 °C, −40 °C, −60 °C, and −80 °C. At 20 °C, the pyrrole resonance is a broad peak, which may be due to the fast rotation of NO about the Fe−NO bond. When cooling to ∼−20 °C, a striking downfield shift occurs accompanying pyrrole splitting to one sharp peak at 9.12 ppm and one broad peak at 8.54 ppm, with integration found to be in a 1:7 ratio. With further cooling, the integration ratio of *sharp peak* versus *broad peak* increases to 2:6 (at −40 °C), 3:5 (at −60 °C), and 4:4 (at −80 °C). This trend is in accordance with a slowing of the NO rotation or even a "sitting" oxygen atom behavior. Especially at −80 °C, four pyrrole protons were expected to be in the exact same magnetic environment, and another four pyrrole protons stayed in a very similar environment, due to two equally occupied NO orientations at low temperatures, as Scheidt and coworkers[49] suggested in the crystalline phase studies of (TPP)Fe(NO). The assignments of these peaks as pyrrole resonances were also confirmed by ^2H NMR spectroscopy employing a deuteriated heme complex, $(F_8\text{-}d_8)Fe(NO)$ (see Figure S6, Supporting Information).

Table 2. ^1H NMR Spectroscopic Resonance Comparison: Heme−Fe Mono- and Dinitrosyl Complexes (CD_2Cl_2 at RT)

heme−Fe complex	*pyrrole*-H (ppm)	*meta*-H (ppm)	*para*-H (ppm)	ref
(TPP)Fe(NO)	5.95	8.25	7.45	40
(TMP)Fe(NO)	5.79	8.42/8.22		40
$(F_8)Fe(NO)$	6.00	8.17	7.65	40
$(OEP)Fe(NO)^a$		8.2	6.7	43
$(OEP)Fe(NO)_2{}^a$	8.94	7.39	7.19	43
$(F_8)Fe(NO)$	6.05	8.18	7.67	this work
$(F_8)Fe(NO)^b$	9.12/8.54	7.45	7.86	this work
$(F_8)Fe(NO)_2{}^b$	9.13/8.93	7.45	7.85	this work

[a] Spectra recorded in toluene-d_7. [b] Spectra recorded at −80 °C.

The ^1H NMR spectrum of what was thought to be $(F_8)Fe(NO)_2$, as recorded at −80 °C, presents what appears to be a symmetrically split signal for the pyrrole protons (Figure 4). However, the peak at 9.13 ppm overlaps exactly with that of the mononitrosyl species $(F_8)Fe(NO)$, indicating that a mixture is present and that the 8.93 ppm signal can be assigned to the dinitrosyl species. With warming to −60 °C and −40 °C, ^1H NMR spectra (Figure S7, Supporting Information) indicate that a mixture of $(F_8)Fe(NO)_2$ and $(F_8)Fe(NO)$ is present, but with less dinitrosyl complex present. The 8.93 ppm signal diminishes and shifts/broadens. At RT, the mononitrosyl

(49) Silvernail, N. J.; Olmstead, M. M.; Noll, B. C.; Scheidt, W. R. *Inorg. Chem.* **2009**, *48*, 971–977.

Figure 4. ^{1}H NMR spectra recorded in CD_2Cl_2. Top: $(F_8)Fe(NO)$, RT. Middle: $(F_8)Fe(NO)$ at −80 °C. Bottom: $(F_8)Fe(NO)_2$ at −80 °C. The peak at 5.32 ppm is CD_2Cl_2.

complex fully reforms.[50] These results indicate that, under the conditions of the ^{1}H NMR experiment, with the concentrations of heme and the amount of $NO_{(g)}$ that could be added to the sample tube, $(F_8)Fe(NO)_2$ is not fully formed. This is unlike what the situation appears to be in the separate UV−vis and EPR spectroscopy experiments (vide supra), where full formation is indicated.

A number of heme dinitrosyl complexes have been previously described, and there has been increased interest in such species. In 1974, Wayland and Olson[51] suggested that a dinitrosyl complex forms from the reversible coordination of $\bullet NO_{(g)}$ to (TPP)Fe(NO) in toluene. The compound was suggested to be a $(TPP)Fe^{II}(NO^-)(NO^+)$ species, that is, with a linear $Fe^{II}-NO^+$ unit and a bent $Fe^{II}-NO^-$ unit. In an electrochemical study in 1983, Kadish and Lancon[52] suggested that the formation of $(OEP)Fe(NO)_2$ (OEP = octaethylporphyrin) and $(TPP)Fe(NO)_2$ occurs under $\bullet NO_{(g)}$ pressure and that these could be electrochemically oxidized to cationic species. Ford and Lorkovic[43] pointed out that the optical spectrum for that TPP complex more resembled that of a nitrosyl/nitrito complex. In 2000, Ford and Lorkovic[43] described the dinitrosyl compounds $Fe(TmTP)(NO)_2$ (TmTP = *meso*-tetra-*m*-tolyl-porphinato dianion) and $Fe(TPP)(NO)_2$, using cryogenic conditions to stabilize the binding of a second NO; the adducts were characterized by UV−vis, IR, and NMR spectroscopies. Fe(TmTP)(NO) displays $\nu_{(N-O)}$ = 1683 cm^{-1}; $Fe(TmTP)(NO)_2$ also possesses a single N−O stretch, $\nu_{(N-O)}$ = 1696 cm^{-1}.

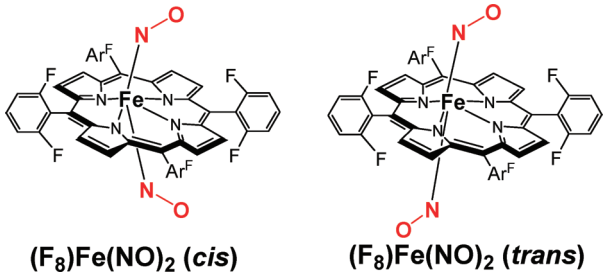

Figure 5. Two possible conformations (cis, trans) of the present $(F_8)Fe(NO)_2$ complex. Both have been suggested, but DFT calculations in 2003 from the groups of both Ford[58] and Ghosh[59,60] support the view that the cis configuration would be the preferred structure in a porphyrinate−iron environment.

In more biological situations, a *trans*-dinitrosyl species had been suggested to occur during $(NO)Fe^{III}$ hemoglobin autoreduction chemistry,[53] while to explain $\bullet NO_{(g)}$-dependent behavior during s-guanylate cyclase (sGC) activity, Ballou and co-workers[54] at one point raised the possibility of such an entity forming. Since then, biophysical[55,56] and theoretical studies[57] on cytochrome *c*′ (cyt. *c*′), bacterial class II cytochromes perhaps involved in $\bullet NO_{(g)}$ detoxification, led to suggestions that its heme may bind two NO's. As there are similarities between cyt. *c*′ and sGC (e.g., they both bind NO but not O_2),[57] the cyt. *c*′ researchers have supported the view that a $Fe(NO)_2$ species may form as a transient intermediate in sGC.

In fact, two computational studies[58−60] carried out have led to a proposed heme dinitrosyl complex structure, both suggesting a lowest-energy "trans−syn" conformation,[59,60] what we refer to here as the "cis"[58] conformation, Figure 5. Here, the nitrosyl ligands reside on opposite sides of the heme and the NO groups are bent over in the same direction. While Ford and Lorkovic[43] only observed a single pyrrole resonance for $Fe(TmTP)(NO)_2$, it is notable that here we observe two types of protons for $(F_8)Fe(NO)_2$ at −80 °C, Figure 4. However, these data still cannot differentiate between two possible structures, the "cis" versus the "trans" configuration (Figure 5).

To summarize, we have observed here the reversible formation of $(F_8)Fe(NO)_2$ from a $\bullet NO_{(g)}$ reaction with $(F_8)Fe(NO)$, as deduced via UV−vis, EPR, and NMR

(50) ^{1}H NMR spectra of $(F_8)Fe(NO)_2$ and $(F_8)Fe(NO)$ in acetone-d_6 are also given in the Supporting Information.

(51) Wayland, B. B.; Olson, L. W. *J. Am. Chem. Soc.* **1974**, *96*, 6037–6041.
(52) Lancon, D.; Kadish, K. M. *J. Am. Chem. Soc.* **1983**, *105*, 5610–5617.
(53) Addison, A. W.; Stephanos, J. J. *Biochemistry* **1986**, *25*, 4104–4113.
(54) Zhao, Y.; Brandish, P. E.; Ballou, D. P.; Marletta, M. A. *Proc. Natl. Acad. Sci.* **1999**, *96*, 14753–14758.
(55) Lawson, D. M.; Stevenson, C. E. M.; Andrew, C. R.; Eady, R. R. *Embo. J.* **2000**, *19*, 5661–5671.
(56) Pixton, D. A.; Petersen, C. A.; Franke, A.; van Eldik, R.; Garton, E. M.; Andrew, C. R. *J. Am. Chem. Soc.* **2009**, *131*, 4846–4853.
(57) Marti, M. A.; Capece, L.; Crespo, A.; Doctorovich, F.; Estrin, D. A. *J. Am. Chem. Soc.* **2005**, *127*, 7721–7728.
(58) Patterson, J. C.; Lorkovic, I. M.; Ford, P. C. *Inorg. Chem.* **2003**, *42*, 4902–4908.
(59) Conradie, J.; Wondimagegn, T.; Ghosh, A. *J. Am. Chem. Soc.* **2003**, *125*, 4968–4969.
(60) Ghosh, A. *Acc. Chem. Res.* **2005**, *38*, 943–954.

Table 3. UV−Vis Comparison of Relevant (F_8)−Fe Complexes

complex	THF (λ_{max}, nm)	acetone (λ_{max}, nm)
$(F_8)Fe(NO)$	410 (Soret), 546	399 (Soret), 541
$(F_8)Fe(NO)_2$	410 (Soret), 540	426 (Soret), 538
$[(F_8)Fe^{III}]SbF_6$	394 (Soret), 510	404 (Soret), 510, 568
products of $\{(F_8)Fe(NO)_2 + (tmpa)Cu(MeCN)]^+ + 2\ H^+\}$	394 (Soret), 510	404 (Soret), 510, 568
products of $\{(F_8)Fe(NO)_2 + (tmpa)Cu(MeCN)]^+\}$	410 (Soret), 546	399 (Soret), 541

spectroscopic studies.[61] Future investigations will be directed at understanding more about the electronic structure of $(F_8)Fe(NO)_2$ or analogs (such as studying Mössbauer spectroscopic properties), the detailed nature of the equilibrium between it and its mononitrosyl precursor, and the reactivity of $(F_8)Fe(NO)_2$ with nucleophilic or electrophilic substrates. As mentioned above, the dinitrosyl complex has been very useful for us to carry out stoichiometric reactions where only two $\bullet NO_{(g)}$ molecules are present for a heme plus copper complex reaction, as described below.

Reaction of $(F_8)Fe(NO)_2$ with $[(tmpa)Cu^I(MeCN)]^+$ Plus Acid; •NO Reductive Coupling. With the presence of 2 equiv of acid in the form of $H(Et_2O)_2[B(C_6F_5)_4]$ (HBArF), the reductive coupling of nitrogen monoxide was efficiently facilitated by this heme and copper complexes mixture of $(F_8)Fe(NO)_2$ and $[(tmpa)Cu^I(MeCN)]^+$ (Scheme 3A), in the same stoichiometry as is known for C*c*Os:

$$(F_8)Fe^{II} + [(tmpa)Cu^I(MeCN)]^+ + 2NO_{(g)} + 2H^+ \rightarrow [(F_8)Fe^{III}]^+ + [(tmpa)Cu^{II}(MeCN)]^{2+} + N_2O_{(g)} + H_2O \quad (3)$$

Gas chromatography analysis (see the Supporting Information, Figure S11) of the head space of the product mixture revealed a $N_2O_{(g)}$ yield of 84%, based on eq 3 and corresponding to the NOR stoichiometry of $2NO + 2H^+ + 2e^- \rightarrow N_2O + H_2O$. This compares to the 80% yield of gaseous nitrous oxide obtained in the system with a binuclear heme/Cu complex of the ^{6}L ligand (Scheme 2);[1] both the binuclear complex and present component (heme + copper complex) system efficiently effect the NOR chemistry.

In order to rule out the possibility that only $(F_8)Fe(NO)_2$ itself mediates the •NO reductive coupling observed, its reaction with 2 equiv of acid (HBArF) in a cold acetone solution was investigated. No UV−vis change was observed at low temperatures, even following warming from −80 °C. The iron(II) nitrosyl complex $(F_8)Fe(NO)$ was produced as determined by UV−vis, IR, and EPR spectroscopic analysis; $\bullet NO_{(g)}$ was released as detected by GC analysis. This control experiment indicates that only $(F_8)Fe(NO)_2$ and acid cannot facilitate NO reductive coupling; that is, the copper complex $[(tmpa)Cu^I(MeCN)]^+$ has a critical role in the NOR chemistry described here.

Identity of Products Formed. Different from the starting material employed, the orange-colored dinitrosyl complex $(F_8)Fe(NO)_2$ forms a homogeneous brown solution upon addition of the copper(I) complex and acid (see the Experimental Section). A UV−vis spectrum of the product mixture has λ_{max} = 394 (Soret) and 510 nm (in THF, Table 3), which corresponds to what should be a heme−Fe^{III} complex $[(F_8)Fe^{III}]^+$ with a $B(C_6F_5)_4^-$ counteranion (see the Experimental Section). In fact, these UV−vis properties perfectly match those of $[(F_8)Fe^{III}]SbF_6$, which was independently synthesized (Table 3). To further determine the identity of the products of the reaction (eq 3), an EPR spectrum was recorded following precipitation of the solids from the reaction mixture in acetone/CH_3CN and redissolution in acetone (Figure 6A). It also confirms the presence of the heme−Fe^{III} species (i.e., $[(F_8)Fe^{III}]^+$) along with a Cu^{II} complex with trigonal bipyramidal (TBP) coordination geometry, possessing well-known (for TBP Cu^{II}) "reverse" axial EPR spectral properties ($g_\perp > g_\parallel$).[62−64] In fact, this perfectly matches the known spectroscopic behavior of $[(tmpa)Cu^{II}(MeCN)]^{2+}$ (see the Experimental Section and Figure 6B). To confirm that the heme and copper products were formed in equal amounts, as per eq 3 and Scheme 3A, we generated and recorded an EPR spectrum of a made-up 1:1 (molar equiv) mixture of $[(F_8)Fe^{III}]SbF_6$ and $[(tmpa)Cu^{II}(MeCN)](ClO_4)_2$, Figure 6B. This beautifully matches the spectrum recorded for the product mixture in the NO reductive coupling reaction (Figure 6A), $(F_8)Fe^{III}$ (g = 6.10) and Cu^{II} ($g_\perp$ = 2.21, $g_\parallel$ = 2.01, $A_\perp$ = 100 G, $A_\parallel$ = 68 G).

To check on other possible products in the reaction mixture, we used the solid material obtained by adding pentane to the acetone/MeCN reaction mixture. An IR spectrum (Nujol mull)[65] showed that there is *no* nitrosyl−heme species present, further corroborating the nature of the reaction; both NO molecules initially present as the $(F_8)Fe(NO)_2$ complex are consumed, and $N_2O_{(g)}$ is produced (vide supra). To check for the possibility that nitrite might have been generated and might have accounted for some product of •NO reactivity, we carried out ion chromatography analysis on an aqueous extract of the reaction mixture (see the Experimental Section). However, no trace of nitrite could be detected. A room-temperature ^{1}H NMR spectrum of the products solution in CD_3CN (Figure 10) showed it was a mixture of what appeared to be a high-spin heme−Fe^{III} complex and also possessing paramagnetically shifted signals ascribed to the TMPA ligand on $[(tmpa)Cu^{II}(MeCN)](ClO_4)_2$

(61) We have thus far been unable to obtain low-temperature infrared spectroscopic data for this complex.

(62) Maiti, D.; Lee, D.-H.; Narducci Sarjeant, A. A.; Pau, M. Y. M.; Solomon, E. I.; Gaoutchenova, K.; Sundermeyer, J.; Karlin, K. D. *J. Am. Chem. Soc.* **2008**, *130*, 6700–6701.

(63) Lucchese, B.; Humphreys, K. J.; Lee, D.-H.; Incarvito, C. D.; Sommer, R. D.; Rheingold, A. L.; Karlin, K. D. *Inorg. Chem.* **2004**, *43*, 5987–5998.

(64) Karlin, K. D.; Hayes, J. C.; Shi, J.; Hutchinson, J. P.; Zubieta, J. *Inorg. Chem.* **1982**, *21*, 4106–4108.

(65) Data not shown.

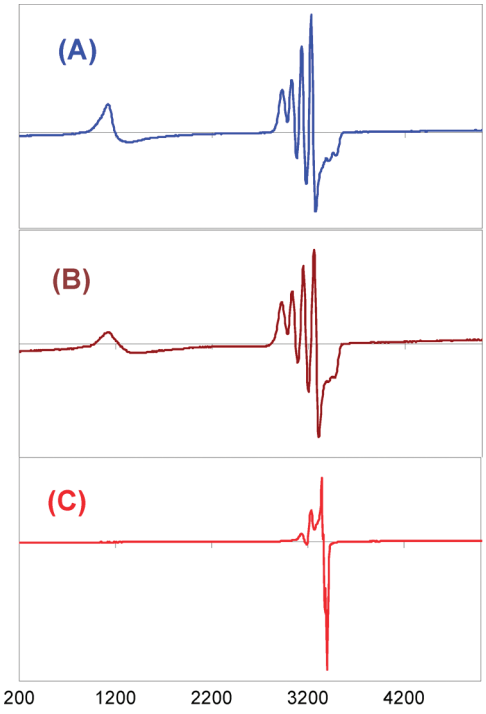

Figure 6. EPR spectra (acetone; 77 K) of (A) the product mixture of the reaction $(F_8)Fe(NO)_2$ + $[(tmpa)Cu^I(MeCN)]^+$ + 2 H^+ (blue) showing the typical heme−Fe^{III} complex and $[(tmpa)Cu^{II}(solvent)]^{2+}$; (B) a madeup 1:1 mixture of $[(F_8)Fe^{III}]SbF_6$ and $[(tmpa)Cu^{II}(MeCN)](ClO_4)_2$ (brown); (C) the product mixture obtained from the reaction of $(F_8)Fe(NO)_2$ + $[(tmpa)Cu^I(MeCN)]^+$ in the absence of acid (red), $(F_8)Fe(NO)$ + $1/3[(tmpa)Cu^{II}(NO_2^-)]^+$ + unreacted $2/3[(tmpa)Cu^I(solvent)]^+$. See Figure S8 (Supporting Information) for an expanded view of this spectrum. See the text for further explanation.

(as determined from the previously determined NMR properties of this complex).[66] A more detailed description of the NMR spectroscopic and spin-state properties of this heme complex, $[(F_8)Fe^{III}]SbF_6$, will be discussed below.

Reaction of $(F_8)Fe(NO)_2$ with $[(tmpa)Cu^I(MeCN)]^+$ in the Absence of Acid. Of course, the presence of protons is required in NORs to give turnover, see eq 1. In fact, we originally hypothesized that we may not need protons to effect •NO reductive coupling. In NORs, it is thought that a μ-oxo heme/nonheme diiron(III) complex forms following reductive coupling, as this has been detected by several groups.[4,11,67−69] Perhaps the chemistry could proceed as follows:

$$\text{heme}-Fe^{II} + Fe_B{}^{II} + 2\bullet NO \rightarrow \text{heme}-Fe^{III}-O-Fe^{III}{}_B + N_2O_{(g)}$$

Thus, we hypothesized that proton equivalents might not be necessary for the same chemistry to occur in heme−copper oxidases, since our research group has synthesized and published on a number of heme−Fe^{III}−O−Cu^{II} complexes, including ones which are structurally characterized.[29,70,71] So, perhaps the heme−iron and copper ions would facilitate $\bullet NO_{(g)}$ coupling chemistry and also be Lewis acidic enough to force this reaction without protons, as

$$\text{heme}-Fe^{II} + Cu^I{}_B + 2\bullet NO_{(g)} \rightarrow \text{heme}-Fe^{III}-O-Cu^{II}{}_B + N_2O_{(g)}$$

However, this is not the case, and as described above, acid is required to effect $\bullet NO_{(g)}$ coupling in the $(F_8)Fe(NO)_2$ + $[(tmpa)Cu^I(MeCN)]^+$ system. In fact, when $[(tmpa)Cu^I(MeCN)]^+$ is added to $(F_8)Fe(NO)_2$ without acid present, the products obtained are a mixture of heme−nitrosyl plus Cu^{II}−nitrite and unreacted Cu^I complexes, eq 4 (and Scheme 3B).

$$(F_8)Fe(NO)_2 + [(tmpa)Cu^I(MeCN)]^+ \rightarrow (F_8)Fe(NO) + 1/3[(tmpa)Cu^{II}(NO_2^-)]^+ + 2/3[(tmpa)Cu^I(solvent)]^+ + 1/3N_2O_{(g)} \quad (4)$$

A UV−vis spectrum of a reaction mixture reveals bands associated with the presence of $(F_8)Fe(NO)$, only λ_{max} (THF) = 410 (Soret) and 546 nm and λ_{max} (acetone) = 399 (Soret) and 541 nm, and IR spectroscopy gives ν_{NO} = 1684 cm^{-1}.[65] An EPR spectrum of the reaction product solution (Figure 6C) indicates that it is a mixture of typical (porphyrinate)Fe^{II}−NO and Cu^{II} species,[72] consistent with our proposed course of reaction (eq 4). Thus, without added acid, one of the two nitrogen monoxide molecules (per heme/Cu stoichiometric mixture) remains within a metal complex product, that is, in the form of $(F_8)Fe(NO)$. Our expectation then was that any remaining •NO released may have undergone a copper complex mediated disproportionation reaction, giving nitrite and $N_2O_{(g)}$ according to well-established copper(I)/$\bullet NO_{(g)}$ chemistry:[4,45]

$$3\bullet NO + [(L)Cu^I]^+ \rightarrow N_2O + [(L)Cu^{II}(NO_2^-)]^+ \quad (5)$$

In fact, this seems to be the case. GC analysis reveals that $N_2O_{(g)}$ is produced in 88% yield on the basis of eq 5. This is far less than should be or is produced by our NOR chemistry with acid present, Scheme 3A and eq 3. In further support of the chemistry outlined here, ion chromatography analysis of an aqueous solution extract of the reaction mixture (see the Experimental Section) indicates that nitrite (NO_2^-) is present in the product mixture with a yield of 95%, according to eq 5. In summary, without added acid, one of the two nitrogen monoxide molecules

(66) Nanthakumar, A.; Fox, S.; Murthy, N. N.; Karlin, K. D. *J. Am. Chem. Soc.* **1997**, *119*, 3898–3906.
(67) Pinakoulaki, E.; Gemeinhardt, S.; Saraste, M.; Varotsis, C. *J. Biol. Chem.* **2002**, *277*, 23407–23413.
(68) Moënne-Loccoz, P.; Richter, O.-M. H.; Huang, H.-w.; Wasser, I. M.; Ghiladi, R. A.; Karlin, K. D.; de Vries, S. *J. Am. Chem. Soc.* **2000**, *122*, 9344–9345.
(69) Field, S. J.; Prior, L.; Roldan, M. D.; Cheesman, M. R.; Thomson, A. J.; Spiro, S.; Butt, J. N.; Watmough, N. J.; Richardson, D. J. *J. Biol. Chem.* **2002**, *277*, 20146–20150.
(70) Ju, T. D.; Ghiladi, R. A.; Lee, D.-H.; van Strijdonck, G. P. F.; Woods, A. S.; Cotter, R. J.; Young, J. V. G.; Karlin, K. D. *Inorg. Chem.* **1999**, *38*, 2244–2245.
(71) Kim, E.; Helton, M. E.; Wasser, I. M.; Karlin, K. D.; Lu, S.; Huang, H.-w.; Moënne-Loccoz, P.; Incarvito, C. D.; Rheingold, A. L.; Honecker, M.; Kaderli, S.; Zuberbühler, A. D. *Proc. Natl. Acad. Sci. U.S.A.* **2003**, *100*, 3623–3628.
(72) The amount of Cu(II) complex present should be at a level of 1/3 of the amount of heme−nitrosyl complex present, see eq 4 thus, the g = 2.0−2.2 region of Figure 6C is dominated by the heme−nitrosyl complex signal

remains in the product, and the other $\bullet NO_{(g)}$ molecule released is disproportionated to nitrite in the form of a nitrito complex and $N_2O_{(g)}$. Further evidence comes from control experiments, where we separately show that $[(tmpa)Cu^I]^+$ is a complex which does facilitate nitrogen monoxide disproportionation, see below.

Reaction of $[(tmpa)Cu^I(MeCN)]^+$ with $\bullet NO_{(g)}$; Nitrogen Monoxide Disproportionation[4,45]**.** When excess $\bullet NO_{(g)}$ is exposed to $[(tmpa)Cu^I(MeCN)]^+$, the related nitrito complex $[(tmpa)Cu^{II}(NO_2)]^+$ is produced in excellent yield, as determined by elemental analysis and UV−vis and EPR spectroscopies (Figures S2 and S3, Supporting Information) and ion chromatography, which was carried out to further confirm/identify the nitrite anion (see the Experimental Section). Nitrous oxide gas was also identified qualitatively (by GC); quantitative determination was made difficult by the conditions of excess •NO(g) required to obtain high yields of $[(tmpa)Cu^{II}(NO_2)]^+$. To summarize, $[(tmpa)Cu^I(MeCN)]^+$ is capable of $\bullet NO_{(g)}$ disproportionation chemistry and is likely the source of $N_2O_{(g)}$ when $[(tmpa)Cu^I(MeCN)]^+$ reacts with $\bullet NO_{(g)}$, by itself (as described here), or in the reaction also with $(F_8)Fe(NO)_2$ present but without added acid (vide supra).

Structure, Spectroscopy, and Spin-State Properties of $[(F_8)Fe^{III}](SbF_6)$. As described above, $[(F_8)Fe^{III}]^+$ (as the $B(C_6F_5)_4$ salt) was formed in the NOR model system reacting $(F_8)Fe(NO)_2$ with $[(tmpa)Cu^I(CH_3CN)]^+B(C_6F_5)_4^-$ in the presence of acid. And to help confirm its identity, we separately synthesized $[(F_8)Fe^{III}]SbF_6$ via a metathesis reaction of $(F_8)Fe^{III}Cl$ with $AgSbF_6$ (see the Experimental Section and Figure S9, Supporting Information), and we compared UV−vis and EPR properties with those obtained in our NOR model reaction. However, a closer examination of the EPR and NMR properties of $[(F_8)Fe^{III}]SbF_6$ indicates that the complex exists as a spin-state mixture of $S = 3/2$ and $S = 5/2$, with the ground state being mainly a high-spin state ($S = 5/2$). The following paragraphs detail this situation.

There is extensive literature concerning spin states which can occur with iron(III) porphyrinate complexes.[48,73] High-spin, intermediate-spin, or low-spin states which occur are dramatically influenced by the external ligand(s) bound to the heme. A variety of physical techniques can be applied to characterize and differentiate spin-state possibilities for heme−Fe^{III} complexes, such as X-ray crystallography along with EPR and NMR spectroscopies. One of the principal structural features is the $M-N_{porphyrinate}$ bond length, which increases as one goes from lower to higher spin states, that is, $S = 1/2 < S = 3/2 < S = 5/2$. Second, g values observed in EPR spectra become enlarged when the spin states are higher. Third, ^1H NMR spectra exhibit notable downfield shifts of the pyrrole protons when the spin states change from low to intermediate to high spin. Certain heme−Fe^{III} complexes are known to possess an admixture (but not thermal equilibrium) of $S = 3/2$ and $S = 5/2$ species, and these exhibit a range of physical properties.[48,73]

In fact, a good number of $[(porphyrinate)Fe^{III}]^+$ complexes, such as five-coordinated $[(TPP)Fe^{III}]ClO_4$, are known to be spin-admixed complexes,[35] also see Table 4. Walker and co-workers[74] have in fact previously studied $[(F_8)Fe^{III}]ClO_4$; in CH_2Cl_2, this was shown to be an $S = 3/2$ and $S = 5/2$ spin admixture. The ground state was largely high-spin with the $S = 3/2$ state as the first excited state, on the basis of EPR (4.2 K) and NMR (CD_2Cl_2) spectroscopic properties. Here, we compare these properties with our own $[(F_8)Fe^{III}]SbF_6$ in CH_2Cl_2. As we were able to obtain crystals and an X-ray structure of $[(F_8)Fe^{III}(THF)_2]SbF_6$ (vide infra), we also more carefully examined this six-coordinated species' THF solution EPR (77 K) and variable-temperature NMR spectroscopic properties. As described below, we also find both $[(F_8)Fe^{III}]SbF_6$ and $[(F_8)Fe^{III}(THF)_2]SbF_6$ complexes to be an $S = 3/2$ and $S = 5/2$ spin admixture.

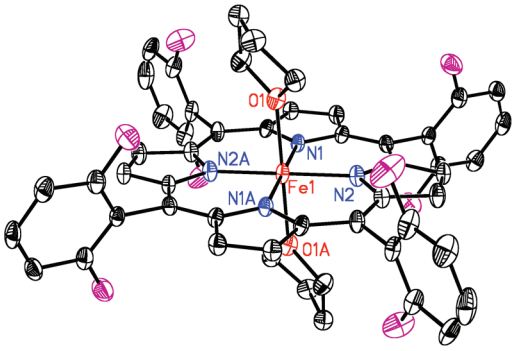

Figure 7. ORTEP diagram showing the cationic portion of of $[(F_8)Fe^{III}(THF)_2]SbF_6$. Also see Table 4 for structural parameters.

Recrystallization of isolated complex $[(F_8)Fe^{III}]SbF_6$ out of THF/hexane provides a bis-THF complex, $[(F_8)Fe^{III}(THF)_2]SbF_6$ (see the Experimental Section and Supporting Information); the structure is depicted in Figure 7. The average $Fe-N_{porphyrinate}$ bond distance is 2.027 (3) Å, clearly between those of known low-spin (avg. = ∼1.99 Å) and high-spin six-coordinate derivatives (avg. > 2.04 Å). Also see Table 4 for these and other relevant comparisons. The value is also much shorter

(73) Scheidt, W. R. *Porphyrin Hand.* **2000**, *3*, 49–112.

(74) Nesset, M. J. M.; Cai, S.; Shokhireva, T. K.; Shokhirev, N. V.; Jacobson, S. E.; Jayaraj, K.; Gold, A.; Walker, F. A. *Inorg. Chem.* **2000**, *39*, 532–540.
(75) Balch, A. L.; Lamar, G. N.; Latosgrazynski, L.; Renner, M. W. *Inorg. Chem.* **1985**, *24*, 2432–2436.
(76) Whitlock, H. W.; Hanauer, R.; Oester, M. Y.; Bower, B. K. *J. Am. Chem. Soc.* **1969**, *91*, 7485.
(77) Scheidt, W. R.; Finnegan, M. G. *Acta Crystallogr., Sect. C* **1989**, *45*, 1214–1216.
(78) Hoard, J. L.; Cohen, G. H.; Glick, M. D. *J. Am. Chem. Soc.* **1967**, *89*, 1992.
(79) Dolphin, D. H.; Sams, J. R.; Tsin, T. B. *Inorg. Chem.* **1977**, *16*, 711–713.
(80) Masuda, H.; Taga, T.; Osaki, K.; Sugimoto, H.; Yoshida, Z.; Ogoshi, H. *Inorg. Chem.* **1980**, *19*, 950–955.
(81) Mylrajan, M.; Andersson, L. A.; Sun, J.; Loehr, T. M.; Thomas, C. S.; Sullivan, E. P.; Thomson, M. A.; Long, K. M.; Anderson, O. P.; Strauss, S. H. *Inorg. Chem.* **1995**, *34*, 3953–3963.
(82) Scheidt, W. R.; Cohen, I. A.; Kastner, M. E. *Biochemistry* **1979**, *18*, 3546–3552.
(83) Cheng, B. S.; Scheidt, W. R. *Acta Crystallogr., Sect. C* **1995**, *51*, 1271–1275.
(84) Higgins, T. B.; Safo, M. K.; Scheidt, W. R. *Inorg. Chim. Acta* **1990**, *178*, 261–267.
(85) Cheng, B.; Safo, M. K.; Orosz, R. D.; Reed, C. A.; Debrunner, P. G.; Scheidt, W. R. *Inorg. Chem.* **1994**, *33*, 1319–1324.
(86) Masuda, H.; Taga, T.; Osaki, K.; Sugimoto, H.; Yoshida, Z.; Ogoshi, H. *Bull. Chem. Soc. Jpn.* **1982**, *55*, 3891–3895.
(87) Serr, B. R.; Headford, C. E. L.; Anderson, O. P.; Elliott, C. M.; Spartalian, K.; Fainzilberg, V. E.; Hatfield, W. E.; Rohrs, B. R.; Eaton, S. S.; Eaton, G. R. *Inorg. Chem.* **1992**, *31*, 5450–5465.

Table 4. Selected Fe−N Bond Distances, g Values, and ^{1}H NMR of heme−Fe^{III} Complexes[a]

heme−Fe^{III}complex	Fe−N (Å)	$g_\perp$ value	pyrrole-H (δ, ppm)	spin state	reference
		Five-Coordinate			
(OEP)FeCl	2.063	5.76 (toluene)	80.3 ($CDCl_3$)	h.s.[b]	73, 75, 76
(TPP)FeCl	2.040 (9) 2.070 (9)	5.66 (toluene)	80.8 (toluene-d_8)	h.s.	75, 77, 78
(F_8)FeCl	2.089(4)	6.16 (CH_2Cl_2)	81.0 ($CDCl_3$)	h.s.	29, 30
[(OEP)Fe](ClO_4)	1.994(10)	5.83 (CH_2Cl_2)		i.s.[c]	79,80
[(TPP)Fe](ClO_4)	2.001(5)	4.72 (CH_2Cl_2), 5.84 (2-metTHF)	−10	h.s. + i.s.	35, 74
[(F_8)Fe](ClO_4)		5.72 (CH_2Cl_2)	∼15	h.s. + i.s.	74
[(F_8)Fe](SbF_6)		5.84 (CH_2Cl_2)	27.2, 11.6	h.s. + i.s.	this work
		Six-Coordinate			
[(OEP)Fe(DMSO)$_2$]$^+$	2.035(9)			h.s.	81
[(TPP)Fe(H_2O)$_2$]$^+$	2.045(8) 2.029(5)	∼6 (solid)		h.s.	82, 83
[(OEP)Fe(1-MeIm)$_2$]$^+$	2.004(2)			l.s.[d]	81
[(TPP)Fe(1-MeIm)$_2$]$^+$	1.982(3)	g_z = 2.890, g_y = 2.291, g_x = 1.554		l.s.	84
[(OEP)Fe(THF)$_2$]$^+$	1.999(2) 1.978(12)	4.68 (CH_2Cl_2)		i.s.	85, 86
[(TPP)Fe(THF)$_2$]$^+$[e]	2.00(1)			i.s.	87
[(F_8)Fe(THF)$_2$](SbF_6)	2.027(3)	6.12 (THF)	54.7, 14.8	h.s + i.s.	this work

[a] OEP = octaethylporphine; TPP = meso-tetraphenylporphyrin; 2-metTHF = 2-methytetrahydrofuran; 1-MeIm = 1-methylimidazole; DMSO = dimethyl sulfoxide. [b] h.s. = high spin, S = 5/2. [c] i.s. = intermediate spin, S = 3/2. [d] l.s. = low spin, S = 1/2. [e] Derived from a dinuclear heme−Fe^{III}−Cu^{II} complex, [(TPP)Fe(THF)$_2$]−{[(TPP)Fe(THF)][Cu(MNT)$_2$]} ·2THF (MNT = *cis*-1,2-dicyanoethylenedithiolate).

than that of the related five-coordinated high-spin complex (F_8)Fe^{III}Cl (Fe−$N_{porphyrinate}$ = 2.089(4) Å),[30] the material used to synthesize [(F_8)Fe^{III}(THF)$_2$]SbF_6. In addition, the axial Fe−O_{THF} bond distance, 2.131 Å, is significantly longer than those observed for low-spin state complexes, but very similar to those of two other bis-THF complexes, [(TPP)Fe(THF)$_2$]$^+$ (Fe−O = 2.16 Å) and [(OEP)Fe(THF)$_2$]$^+$ (Fe−O = 2.187 Å; Table 4). As stated, these compounds are known to possess intermediate-spin states. The possibility that [(F_8)Fe^{III}]SbF_6 is not a quantum-admixed spin system, but rather possesses an intermediate-spin system, is ruled out by EPR and NMR spectroscopic information, as described below.

When [(F_8)Fe^{III}]SbF_6, lacking any THF, is dissolved in CH_2Cl_2 and the EPR spectrum recorded at 77 K, a g = 5.84 feature is observed (Figure 8). This lies in the range expected for admixed-spin state complexes (g = 4.2−6) and is not typical for high- (g = ∼ 6.2) or low-spin complexes (g = ∼3.5 or < 3.4).[73] Our g = 5.84 signal also well matches that observed for [(F_8)Fe^{III}]ClO_4 (g = 5.72, 4.2 K).[74] In addition, this EPR spectrum of [(F_8)Fe^{III}]SbF_6 in frozen CH_2Cl_2 is much broader than that of the typical high-spin complex (F_8)Fe^{III}Cl (Figure 8). The broadening has been suggested to be due to a quantum admixed feature.[88] In the strongly coordinating solvent THF, the 77 K EPR spectrum of [(F_8)Fe^{III}(THF)$_2$]SbF_6 indicates that the complex is mostly or all high-spin, based on the observed g = 6.12 (Figure 8). In other words, and according to the criterion put forth by Walker and co-workers[89] along with Maltempo and Moss,[90] $g_\perp = 6(a_{5/2})^2 + 4(b_{3/2})^2$ {where $(a_{5/2})^2$ and $(b_{3/2})^2$ are the coefficients of the high-spin and intermediate-spin states, respectively}, and thus the EPR data suggest that the high-spin state (S = 5/2) is the ground state for both [(F_8)Fe^{III}]SbF_6 and [(F_8)Fe^{III}(THF)$_2$]SbF_6, while the latter is almost completely at this state.

Further, the ^{1}H NMR spectrum of [(F_8)Fe^{III}]SbF_6 and the position of the pyrrole proton resonances indicates the complex to be in a mixed-spin state at RT in CD_2Cl_2, Figure S10 (Supporting Information). Two pyrrole resonances are observed at $\delta_{pyrrole}$ = 27.2 and 11.6 ppm, both typical for intermediate-spin complexes. These shift downfield when the temperature decreases but still lie in the intermediate-spin state range. [(F_8)Fe^{III}]ClO_4 exhibits $\delta_{pyrrole}$ = ∼15 ppm at RT).[74] In THF-d_8, signals for both high spin ($\delta_{pyrrole}$ = 54.7 at RT) and intermediate spin ($\delta_{pyrrole}$ = 14.8 at RT) are observed at all temperatures (Figure 9). However, a greater fraction of high-spin [(F_8)Fe^{III}-(THF)$_2$]SbF_6 species is present at reduced temperatures, $\delta_{pyrrole}$ (high-spin) = 54.7 ppm at RT, shifting to 107 ppm at −80 °C, which is in the high-spin chemical shift region.

To summarize, the ^{1}H NMR spectra are consistent with EPR spectroscopic and X-ray structural parameters; that is, the ground states of both [(F_8)Fe^{III}]SbF_6 and [(F_8)Fe^{III}(THF)$_2$]SbF_6 are high-spin (S = 5/2), while [(F_8)Fe^{III}]SbF_6 has a larger intermediate-spin fraction (S = 3/2) with increasing temperature. As mentioned earlier, a ^{1}H NMR spectrum of the product mixture of {(F_8)Fe$(NO)_2$ + [(tmpa)Cu^I(MeCN)]$^+$ + 2 H^+} in CD_3CN (Figure 10) might suggest that a high-spin [heme−Fe^{III}]$B(C_6F_5)_4$ (vide supra) product is formed, which seems inconsistent with the data just described for the synthetically derived [(F_8)Fe^{III}]SbF_6 (Figure S10, Supporting Information) or [(F_8)Fe^{III}(THF)$_2$]SbF_6 species. While considering the controlling role of exogenous ligands on the spin states of six-coordinate heme−Fe^{III} complexes, it is likely that either a water molecule (produced from the NOR type reaction) or acetonitrile or acetone (from the reaction solvents) binds to (F_8)Fe^{III}, and this results in it being mostly in a high-spin state.

Summary/Conclusions: Implications for NORs

In this report, we have described heme/Cu complex components (in a 1:1 mixture) facilitating •$NO_{(g)}$ reduction to

(88) Gismelseed, A.; Bominaar, E. L.; Bill, E.; Trautwein, A. X.; Winkler, H.; Nasri, H.; Doppelt, P.; Mandon, D.; Fischer, J.; Weiss, R. *Inorg. Chem.* **1990**, *29*, 2741–2749.
(89) Yatsunyk, L. A.; Shokhirev, N. V.; Walker, F. A. *Inorg. Chem.* **2005**, *44*, 2848–2866.
(90) Maltempo, M. M.; Moss, T. H. *Q. Rev. Biophys.* **1976**, *9*, 181–215.

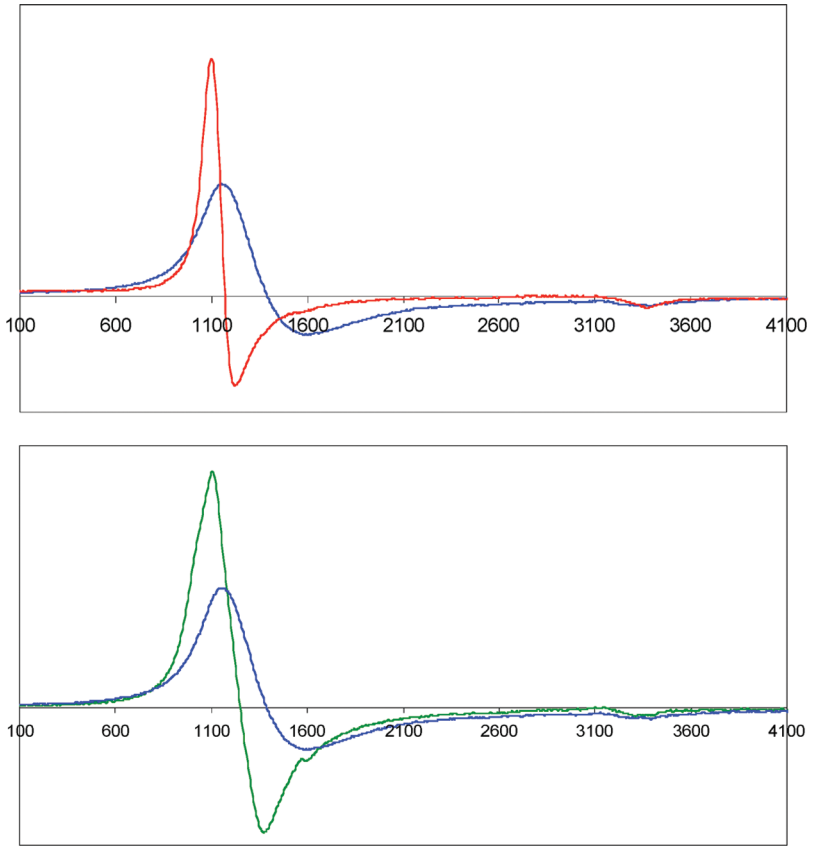

Figure 8. (Top) EPR spectra in CH_2Cl_2 at 77 K of $[(F_8)Fe^{III}]SbF_6$ (blue, $g_\perp = 5.84$) and $(F_8)Fe^{III}Cl$ (red, $g_\perp = 6.16$). (Bottom) EPR spectra of $[(F_8)Fe^{III}]SbF_6$ in two solvents at 77 K, possessing $g_\perp = 5.84$ in CH_2Cl_2 (blue) and $g_\perp = 6.12$ in THF (green) at 77 K.

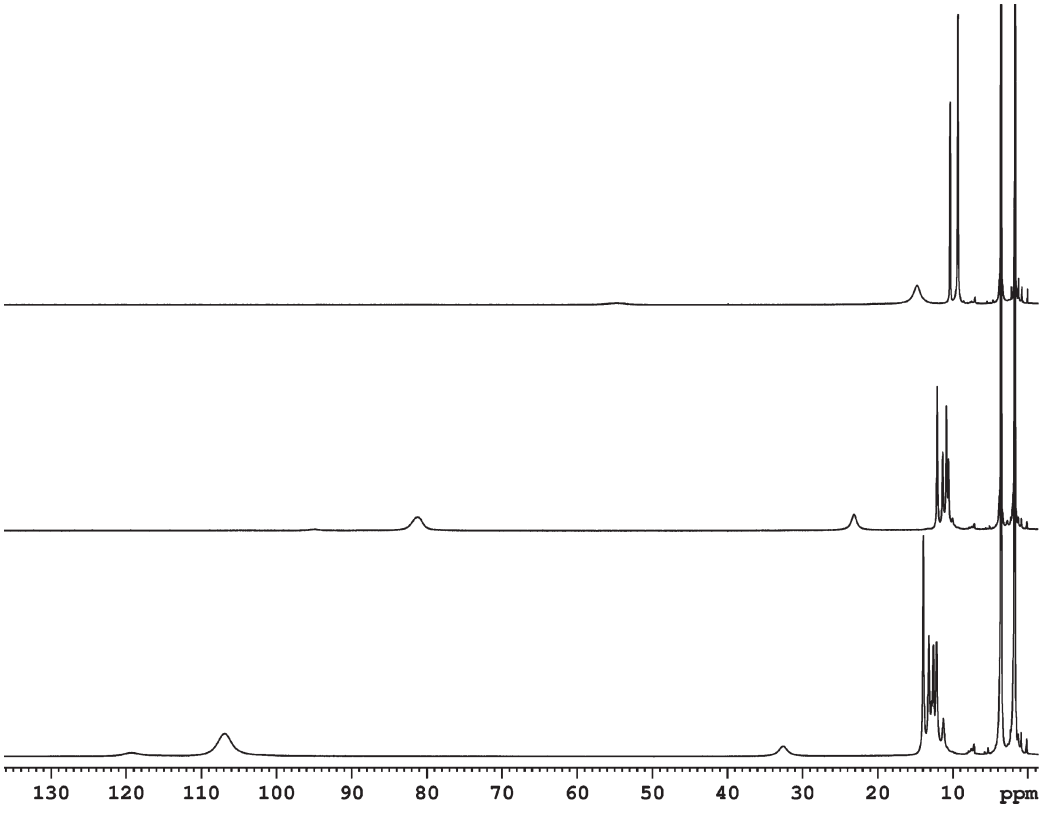

Figure 9. ^1H NMR spectra of $[(F_8)Fe^{III}(THF)_2]SbF_6$ in THF-d_8 at various temperatures: +20, −40, and −80 °C from top to bottom.

$N_2O_{(g)}$, analogous to one enzyme turnover of nitrogen monoxide reactivity with certain C*c*O's. The overall results are not greatly altered from those obtained by instead using a binuclear (^{6}L)-heme/Cu complex (Scheme 2).[1] Heme−Fe^{II},

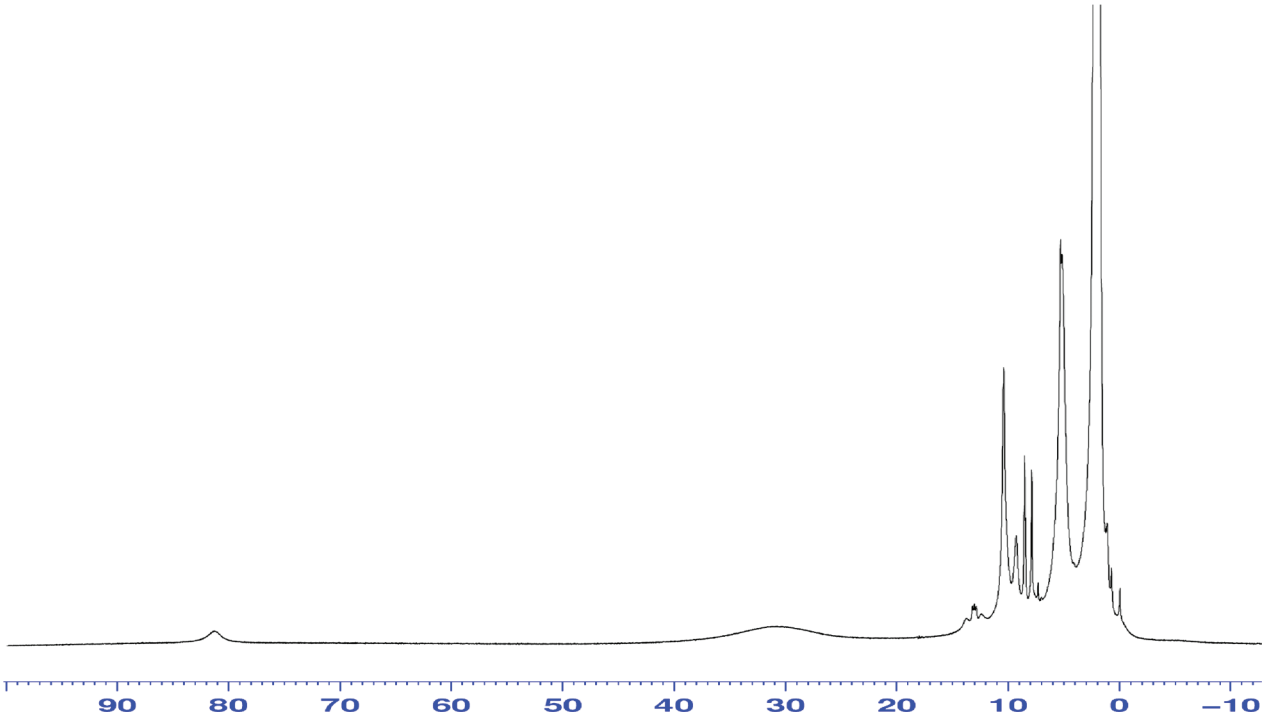

Figure 10. ^{1}H NMR of the product mixture of the NOR reaction: $\{(F_8)Fe(NO)_2 + [(tmpa)Cu^I(MeCN)]^+ + 2\ H^+\}$ in CD_3CN at RT.

Cu^I, and acid are all required to trigger the reaction. The dinitrosyl complex $(F_8)Fe(NO)_2$ provides exactly 2 equiv of •NO per heme-and-copper moiety, allowing us to monitor a stoichiometric reaction. The dinitrosyl complex has been characterized by variable-temperature NMR and UV−vis, as well as EPR spectroscopies. DFT calculations by Ghosh et al.[59,60] and Ford et al.[58] suggest that heme dinitrosyl complexes possess a so-called "cis" conformation, which is in accordance with the ^{1}H NMR spectroscopic data we observe for $(F_8)Fe(NO)_2$. In addition to the five-coordinate $(F_8)Fe(NO)$ complex previously reported, a new six-coordinate complex with THF as the axial base, $(THF)(F_8)Fe(NO)$, was synthesized and characterized by UV−vis, EPR, and IR spectroscopies. Also, $[(F_8)Fe^{III}]SbF_6$, a new variation on previously well-known complexes, was synthesized to help us identify the product of the heme/Cu/$•NO_{(g)}$ chemistry described here, and this has been determined to exist in solution as an admixture of high- and intermediate-spin states.

Concerning heme/Cu $•NO_{(g)}$ reductive coupling (bio)-chemistry, recent biophysical studies and DFT calculations from Varotsis and co-workers[2,13,91,92] have led to the suggestion of what is referred to as a trans mechanism (Scheme 4). This was adopted on the basis of their biophysical and DFT studies, with reference to the literature on heme/nonheme diiron-containing NORs (see the Introduction). Rate-limiting addition of $•NO_{(g)}$ and a proton to heme−nitrosyl complex **II** leads to a "N_2O_2H" intermediate which possesses a N−N bond; note that reduced Cu^I_B is proposed to be present in this species. The oxidized and protonated hyponitrite (deprotonated hyponitrite is $N_2O_2^{2-}$, so **III** would

Scheme 4

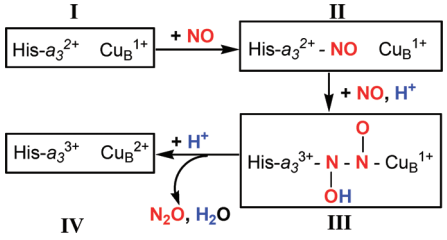

possess a protonated $N_2O_2^-$ moiety, Scheme 4)) is proposed to be N-bound to both the metal ions. These researchers assert direct detection of intermediates **II** and **III** via resonance Raman spectroscopic interrogation;[2,13,91] however, the latter hyponitrite complex was generated by adding excess $•NO_{(g)}$ to an oxidized ($Fe^{III}\cdots Cu^{II}$) form of the enzyme and may be one-electron oxidized from intermediate **III**. Finally, it is suggested that further protonation leads to N_2O generation, Scheme 4.

In light of this proposed enzyme mechanism (Scheme 4), we suggest possible steps in the chemistry described in the present report. A likely first step in the reaction would be the attack of the copper(I) complex ($[(tmpa)Cu^I(MeCN)]^+$) on the nitrogen monoxide ligand in $(F_8)Fe(NO)_2$; an analogous step probably also occurs when N_2O is produced from the (^{6}L)-heme/Cu system (Scheme 2). This may release one $•NO_{(g)}$ molecule, which now attacks a binuclear heme−Fe^{II}−(NO)−Cu^I species to give something like intermediate **III** (Scheme 4), that is, a hyponitrite-type species. Protonation, electron-transfer from Cu^+ of the $(tmpa)Cu^I$ moiety, and N−O cleavage could give $N_2O_{(g)}$ and water, and in our case the heme−Fe^{III} and Cu^{II} complexes observed. We suggest that there are other possibilities that should be considered here, and for other synthetic systems to be studied in the future, or even for the enzymes, see below.

(91) Pinakoulaki, E.; Ohta, T.; Soulimane, T.; Kitagawa, T.; Varotsis, C. *J. Am. Chem. Soc.* **2005**, *127*, 15161–15167.
(92) Ohta, T.; Kitagawa, T.; Varotsis, C. *Inorg. Chem.* **2006**, *45*, 3187–3190.

The likelihood of N−N coupling occurring from a Fe−N−O···O−N−Cu species would seem to us to be problematic. Moënne-Loccoz et al.[12] recently suggested that transient binding of NO to the copper ion may occur as either an O-bound (η^1-O) or a side-on (η^2-NO) complex, as supported by FTIR and resonance Raman spectroscopic studies. Such a situation could lead to a geometry or juxtaposition of the two NO moieties so as to greatly facilitate N−N formation. Further, Moënne-Loccoz et al.[12] suggest that the hyponitrite moiety is O-bound to both heme and copper ion metal centers, contrary to what is suggested by Scheme 4. Related to this hypothesis, Richter-Addo and co-workers[93] recently isolated a stable hyponitrite-bridged diiron(III) complex (OEP)Fe−(*trans*-$^-$ON=NO$^-$)−Fe(OEP). An X-ray structure revealed hyponitrite dianion O,O′ ligation. Protonation of this species led to Fe−O and O−N bond cleavage and a release of $N_2O_{(g)}$.

Thus, more efforts are needed to investigate the catalytic mechanism of this $\bullet NO_{(g)}$ reductive coupling chemistry in C*c*O's. For this present system or analog synthetic systems we design in the future, investigations will be directed toward a number of goals. We wish to find or stabilize a possible hyponitrite or other intermediate(s) that may form and deduce details of the coordination chemistry involved. What is the role of iron versus copper in NO binding and stabilization of a hyponitrite intermediate via O or N ligation? Does electron transfer to two NO molecules occur from both metals together to give ligated $N_2O_2^{2-}$ or a protonated derivative? Or is the process stepwise, one-electron at a time, as suggested in Scheme 4? What is the role and timing of proton addition? How does an axial base (proximal histidine to heme Fe) function during the whole process? Note that we did not have a strong "base" for the heme in the present system, nor for that based on the ^{6}L heterobinuclear complex reported earlier.[1] For the proteins, Varotsis and co-workers suggest that initial $\bullet NO_{(g)}$ binding to the ferrous heme leads to $Fe-N_{histidine}$ cleavage to give a five-coordinate heme-nitrosyl.[11,91,94,95] And of course, there are many basic questions to probe in heme/copper (or heme/nonheme diiron) model systems concerning N−N bond formation and N−O cleavage. We look forward to a rich coordination chemistry of these binuclear heme/M systems and nitrogen oxide species.

Acknowledgment. This work was supported by a grant from the National Institutes of Health (K.D.K., GM 60353) and Korea WCU-Program R31-2008-000-10010-0 (K. D. K.).

Note Added after ASAP Publication. This article was released on December 23, 2009, with errors in the Figure 6 caption and another minor text error. The correct version was posted on January 11, 2010.

Supporting Information Available: X-ray structure CIF file; UV−vis, EPR, and NMR spectroscopic details. This material is available free of charge via the Internet at http://pubs.acs.org.

(93) Xu, N.; Campbell, A. L. O.; Powell, D. R.; Khandogin, J.; Richter-Addo, G. B. *J. Am. Chem. Soc.* **2009**, *131*, 2460–2461.
(94) Stavrakis, S.; Pinakoulaki, E.; Urbani, A.; Varotsis, C. *J. Phys. Chem. B* **2002**, *106*, 12860–12862.
(95) Pinakoulaki, E.; Stavrakis, S.; Urbani, A.; Varotsis, C. *J. Am. Chem. Soc.* **2002**, *124*, 9378–9379.